The female-specific VC neurons are mechanically activated, feed-forward motor neurons that facilitate serotonin-induced egg laying in *C. elegans*

Richard J. Kopchock III[1], Bhavya Ravi[1,2,3], Addys Bode[1], & Kevin M. Collins[1,2,4]

[1]Department of Biology, University of Miami, Coral Gables, FL 33143 USA

[2]Neuroscience Program, University of Miami School of Medicine, Miami, FL, 33136 USA

[3] Present address: Department of Neurology, Johns Hopkins University School of Medicine, Baltimore, MD USA

[4]To whom correspondence should be addressed:

kevin.collins@miami.edu

Department of Biology

University of Miami

1301 Memorial Drive

Coral Gables, FL 33143

Tel: (305) 284-9058

Abstract

Successful execution of behavior requires the coordinated activity and communication between multiple cell types. Studies using the relatively simple neural circuits of invertebrates have helped to uncover how conserved molecular and cellular signaling events shape animal behavior. To understand the mechanisms underlying neural circuit activity and behavior, we have been studying a simple circuit that drives egg-laying behavior in the nematode worm *C. elegans*. Here we show that the female-specific, Ventral C (VC) motoneurons are required for vulval muscle contractility and egg laying in response to serotonin. Ca^{2+} imaging experiments show the VCs are active during times of vulval muscle contraction and vulval opening, and optogenetic stimulation of the VCs promotes vulval muscle Ca^{2+} activity. However, while silencing of the VCs does not grossly affect steady-state egg-laying behavior, VC silencing does block egg laying in response to serotonin and increases the failure rate of egg-laying attempts. Signaling from the VCs facilitates full vulval muscle contraction and opening of the vulva for efficient egg laying. We also find the VCs are mechanically activated in response to vulval opening. Optogenetic stimulation of the vulval muscles is sufficient to drive VC Ca^{2+} activity and requires muscle contractility, showing the presynaptic VCs and the postsynaptic vulval muscles can mutually excite each other. Together, our results demonstrate that the VC neurons facilitate efficient execution of egg-laying behavior by coordinating postsynaptic muscle contractility in response to serotonin and mechanosensory feedback.

Introduction

A fundamental goal of neuroscience is to understand the neural basis of behavior (Bargmann & Marder, 2013). Recent work reporting the synaptic wiring diagrams, or connectomes, of nervous systems provides an unprecedented opportunity to study how the nervous system directs animal behavior (Cook et al., 2019; Lerner et al., 2016; Meinertzhagen, 2018). However, there is an emerging concept in the era of connectomes: that the structure of the nervous system is insufficient to predict function (Bargmann, 2012; Batista-García-Ramó & Fernández-Verdecia, 2018). Released neurotransmitters can signal both synaptically and extrasynaptically through distinct receptors to drive short-term and long-term behavior changes (Chase et al., 2004; Donnelly et al., 2013; Koelle, 2018; Pirri et al., 2009). Neuropeptides can be co-released from synapses and signal alongside neurotransmitters (Banerjee et al., 2017; Brewer et al., 2019). Understanding how an assembly of neurotransmitter and neuromodulator signaling events drives the complex pattern of circuit activity is facilitated by direct tests in simple invertebrate animals (Bargmann & Marder, 2013) and those amenable to genetic investigation (Sengupta & Samuel, 2009). Such studies have the potential to reveal conserved neural circuit signaling mechanisms that underlie behavior.

The egg-laying circuit of the nematode worm *C. elegans* provides an ideal model for such a reductionist approach (Figure 1A; W. R. Schafer, 2006). In this circuit, a pair of Hermaphrodite-Specific command Neurons (HSNs) release serotonin and NLP-3 neuropeptides to promote egg-laying behavior (Brewer et al., 2019; Waggoner et al., 1998). Egg laying occurs when the vulval muscles contract in synchrony to open the vulva and allow passage of an egg from the uterus to the outside environment (Collins & Koelle, 2013). Whether serotonin signals to promote the intrinsic electrical excitability of the vulval muscles and/or to modulate input by other neuronal signaling is still not clear. As in mammals, most muscle contraction events in *C. elegans* are

ultimately driven by acetylcholine (ACh; Richmond & Jorgensen, 1999; Trojanowski et al., 2016). Nicotinic acetylcholine receptor (nAChR) agonists promote egg laying, a response that requires nAChRs expressed on the vulval muscles (Kim et al., 2001; Waggoner et al., 2000). However, animals deficient in ACh signaling lay their eggs more frequently, indicating that endogenous ACh inhibits egg laying (Schafer et al., 1996). These contradictory results indicate a complex role for neurotransmitter signaling events within the egg-laying circuit.

The hermaphrodite-specific Ventral C (VC) motoneurons are the primary cholinergic neurons of the egg-laying circuit and make prominent synapses onto the vulval muscles (Duerr et al., 2001; Pereira et al., 2015; White et al., 1986). Despite numerous studies of how the VCs signal, we still do not have a clear understanding of what the VCs actually do. Egg-laying events are always accompanied by a VC Ca^{2+} transient, but not all VC Ca^{2+} transients result in egg release (Collins et al., 2016). ACh mutants are hyperactive for egg laying (Schafer et al., 1996), resembling animals in which VC neuron development has been disrupted by laser ablation or mutation (Bany et al., 2003). This suggests ACh regulation of egg laying is closely associated with VC signaling. The VCs also extend processes along the vulva, leading to the proposal they might also relay mechanosensory or chemosensory feedback in response to vulval opening (Zhang et al., 2008). Thus, VC activity and signaling appears to regulate egg laying through multiple cellular and signaling pathways, but whether the VCs coordinate the egg laying event itself or provide sensory feedback to the rest of the animal in response to egg laying remains stubbornly unclear.

Here we address the function of the VC motoneurons during egg laying. We find that the VCs function within a serotonergic pathway to drive egg laying. The VCs provide excitatory input to convert the initial stages of vulval muscle contraction into a successful egg-laying event. The

VCs achieve this through direct activation in response to vulval muscle excitation and contraction, forming a positive feedback loop until successful egg laying is achieved.

Results

The VC neurons promote egg laying in response to serotonin

The VC neurons release ACh, and animals genetically deficient in ACh show hyperactive egg laying, releasing their embryos prematurely (Bany et al., 2003; Schafer et al., 1996). To test more directly how loss of synaptic transmission from the VC motor neurons affects egg-laying circuit activity and behavior (Figure 1B), we used a modified *lin-11* promoter/enhancer (Bany et al., 2003) to drive transgenic expression of Tetanus Toxin (Jose et al., 2007) and block synaptic transmission from all six VC neurons. Expression of Tetanus Toxin in the VC neurons did not cause any gross defects in steady-state egg accumulation compared to non-transgenic control animals, indicating that the VC neurons are not strictly required for egg laying (compare Figures 1C and 1D, quantified in Figure 1G). In contrast, *egl-1(n986dm)* mutant animals in which the HSNs undergo apoptosis (Trent et al., 1983), showed a dramatic impairment of egg laying, accumulating significantly more embryos (Figures 1E and 1G). Previous studies indicated that laser ablation of both the HSNs and VCs caused additive defects in egg laying (Waggoner et al., 1998). However, transgenic expression of Tetanus Toxin in the VCs in HSN-deficient *egl-1(n986dm)* mutant animals did not significantly enhance their defects in egg laying (Figure 1F and 1G). We have previously shown that wild-type animals lay their first egg around 7 hours after the L4-adult molt, a time when the VCs show their first activity (Ravi, Garcia, et al., 2018). Animals with silenced VCs showed no significant change in the onset of egg laying compared to non-transgenic control animals (Figure 1H). In contrast, the onset of egg laying in *egl-1(n968dm)* mutant animals lacking HSNs is significantly delayed, occurring about 18 hours after becoming adults (Figure 1H). Expression of Tetanus Toxin in the VCs in HSN-deficient animals did not

enhance the delay in egg laying significantly (Figure 1H), consistent with our results measuring steady-state egg accumulation. These results together show that signaling from the VCs is not required for egg-laying behavior to occur.

We next used a drug-treatment approach to explore possible functions of the VC neurons that may not be apparent in animals under standard laboratory conditions. Previous laser ablation experiments indicated that loss of the VC neurons disrupts the induction of egg laying in response to serotonin (Shyn et al., 2003; Waggoner et al., 1998). The HSNs release serotonin which potently stimulates egg laying even in conditions where egg laying is normally inhibited, such as in liquid M9 buffer (Trent et al., 1983) . Serotonin promotes egg laying in M9 buffer in wild-type animals (Figure 1I). We found that transgenic animals expressing Tetanus Toxin in the VCs failed to lay eggs in response to exogenous serotonin (Figure 1I). HSN-deficient *egl-1(n986dm)* mutant animals are egg-laying defective under normal conditions but will still lay eggs in response to exogenous serotonin (Schafer et al., 1996), and this response was suppressed in animals with silenced VCs (Figure 1I). This resistance to exogenous serotonin in VC-silenced animals was not unique to M9 buffer, as transgenic animals placed on serotonin-infused agar also showed a reduced egg-laying response (Figure 1J). Together, these results show that VC neurotransmitter release is required for induction of egg laying by exogenous serotonin.

It was possible that the observed defects in serotonin response caused by VC silencing could be due to impaired circuit development and/or by compensatory changes in circuit activity. Expression from the VC-specific promoter used to drive Tetanus Toxin begins in the L4 stage as the egg-laying circuit is completing development, well before the onset of egg-laying behavior (Ravi, Garcia, et al., 2018). To silence the VCs acutely after circuit development is complete, we transgenically expressed Histamine-gated chloride channels (HisCl) and treated the animals with exogenous histamine (Pokala et al., 2014; Ravi, Garcia, et al., 2018). Histamine silencing

136 of the VCs caused no gross changes in steady-state egg accumulation (Figure 1K), confirming
137 the results with Tetanus Toxin that VC neurotransmission is not required for egg laying.
138 However, acute histamine silencing of the VCs reduced egg laying in response to serotonin in
139 both wild-type and HSN-deficient *egl-1(n986dm)* mutant animals (Figure 1L). Together, these
140 results show that both VC neuron activity and synaptic transmission are dispensable for egg
141 laying under normal growth conditions, but the VCs are required for egg laying in response to
142 exogenous serotonin.

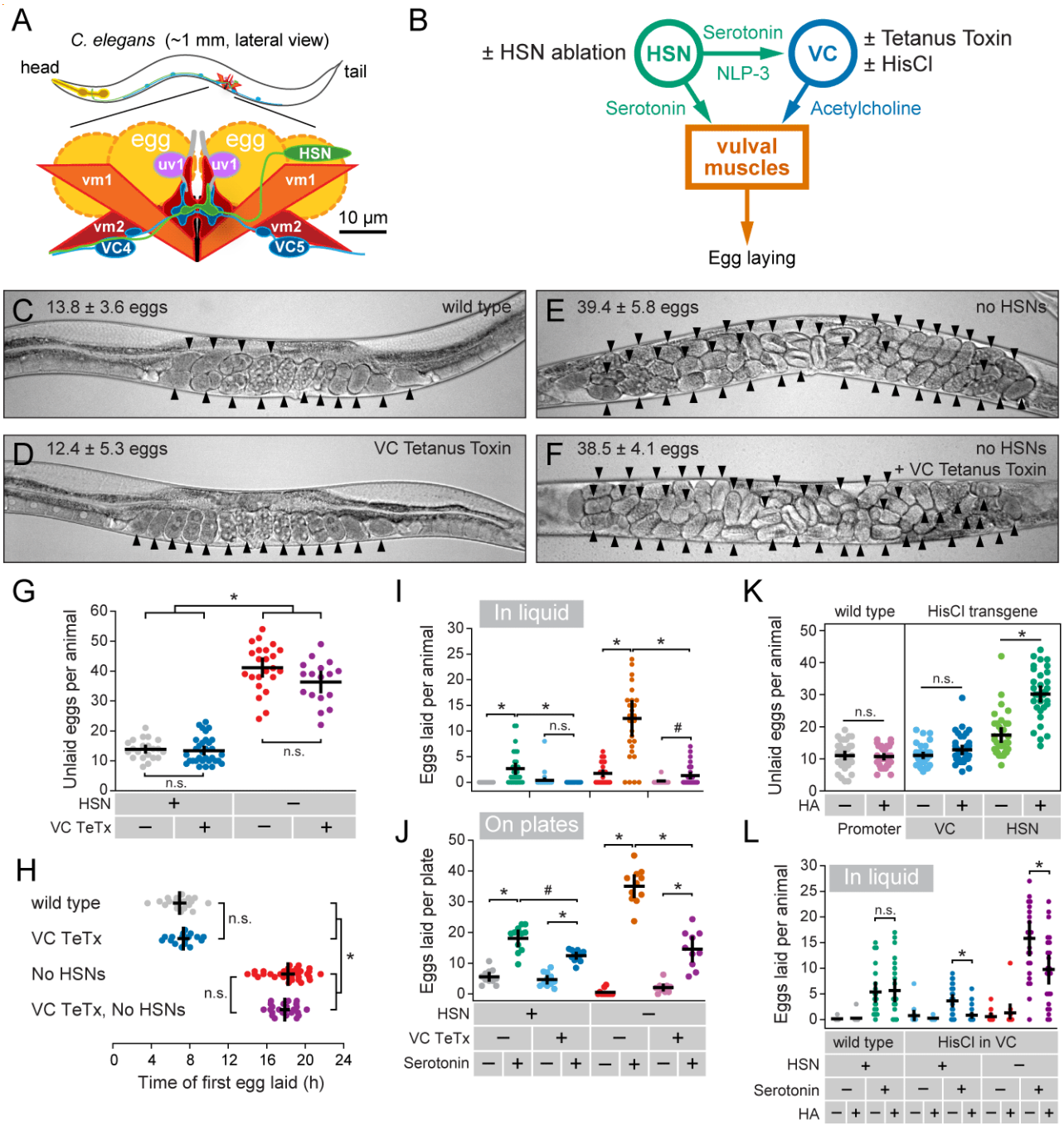

Figure 1. VC neurotransmission is required for serotonin-induced egg laying.

(**A**) Graphical representation of the *C. elegans* egg-laying circuit (Collins et al., 2016). (**B**) Circuit diagram of the synapses and the primary neurotransmitters released between the HSN neurons, VC neurons, and vulval muscles. (**C-F**) Representative images of the *C. elegans* uterus showing unlaid eggs (arrowheads) in wild-type, transgenic animals expressing Tetanus Toxin (TeTx) in the VCs, and HSN-ablated *egl-1(986dm)* mutant animals. (**G**) Scatter plot of unlaid eggs in animals from Figure 1C-F (±95 confidence intervals for the mean); asterisks indicate $p<0.0001$ and n.s. indicates $p>0.05$ (one-way ANOVA with Bonferroni's correction for multiple

comparisons). **(H)** Scatter plot showing timing of first egg laid after the larval to adult molt in animals with blocked VC neurotransmission and ablated HSNs (asterisk indicates $p<0.0001$, one-way ANOVA with Bonferroni's correction for multiple comparisons). (**I**) Blockage of VC synaptic transmission inhibits serotonin-induced egg laying. Animals expressing TeTx in the VCs were placed into M9 buffer or M9 containing 18.5 mM serotonin; asterisks indicate $p\leq0.0002$, pound indicates $p=0.0225$ and n.s. indicates $p>0.05$ (Kruskal-Wallis test with Dunn's correction for multiple comparisons). (**J**) Animals with silenced VCs still fail to lay eggs in response to 18.5 mM serotonin under otherwise normal culturing conditions on plates; asterisks indicate $p<0.0001$, pound indicates $p=0.0026$, and n.s. indicates $p>0.05$ (one-way ANOVA with Bonferroni's correction for multiple comparisons). (**K**) Measurement of steady-state egg accumulation in animals expressing Histamine-gated chloride channels (HisCl) in either the VC or HSN neurons grown with or without histamine; asterisk indicates $p<0.0001$ and n.s. indicates $p>0.05$ (one-way ANOVA with Bonferroni's correction for multiple comparisons). (**L**) Silencing of the VCs blocks serotonin-induced egg laying. Animals expressing HisCl in the VCs were incubated with 0 or 4 mM histamine for four hours, placed into wells with M9 buffer with 0 or 18.5 mM serotonin, and the number of eggs laid after 1 hour were counted; asterisks indicates $p<0.05$ and n.s. indicates $p>0.05$ (Kruskal-Wallis test with Dunn's correction for multiple comparisons).

VC Ca^{2+} activity is coincident with vulval muscle activity and egg laying

The VC neurons show rhythmic Ca^{2+} activity during the egg-laying active state (Collins et al., 2016). However, only ~1/3 of VC Ca^{2+} transients were temporally coincident with vulval muscle contractions that resulted in egg release (Collins et al., 2016), raising questions about the function of the VC Ca^{2+} transients that do not coincide with egg laying. To understand the function of this VC activity we expressed GCaMP5 in the VC neurons to measure Ca^{2+} dynamics in cell bodies and processes most proximal to the vulva while simultaneously recording vulval opening and egg-laying behavior in a separate brightfield channel, as described (Collins & Koelle, 2013). As expected, we found vulval openings that result in egg release were nearly always accompanied by a VC Ca^{2+} transient, but not every VC Ca^{2+} transient resulted in an egg-laying event (Figure 2B; Movie 1). These remaining VC Ca^{2+} transients were almost always observed with partial opening of the vulva (Figure 2C). As quantified in Figure 2F, we found that 48% of VC Ca^{2+} transients were associated with weak vulval openings we termed twitches (Collins & Koelle, 2013) and 39% of VC Ca^{2+} transients were associated with strong openings

that supported egg release. To determine if presynaptic HSN activity was sufficient to drive VC and vulval muscle activity downstream, we optogenetically stimulated HSNs transgenically expressing Channelrhodopsin-2 and simultaneously recorded VC Ca^{2+} activity and vulval muscle contractility (Figure 2A; Movie 2). Optogenetic stimulation of HSNs drove a robust increase in VC Ca^{2+} transients that were associated with egg-laying events, but we still observed VC Ca^{2+} transients during the weaker vulval muscle twitching contractions (Figure 2D). HSN optogenetic stimulation elevated average Ca^{2+} levels in the VCs rapidly, within 5 seconds after blue light exposure (Figure 2E). The light-dependent increase in VC Ca^{2+} activity and vulval muscle contractions were not observed in animals grown without the essential cofactor, all-trans-retinal (ATR; Figure 2D and 2E). During optogenetic HSN activation, 60% of VC Ca^{2+} transients were associated with egg-laying events while only 35% were associated with vulval muscle twitches, a significant difference from control animals not subjected to HSN optogenetic stimulation that we attribute to an increase in egg laying frequency (Figure 2F). Because VC Ca^{2+} activity rises at the same time as vulval opening and prior to egg release, these results are consistent with a model where either the VCs promote vulval muscle contractility and vulval opening, or a model where the VCs are activated in response to downstream vulval muscle contraction and/or vulva opening.

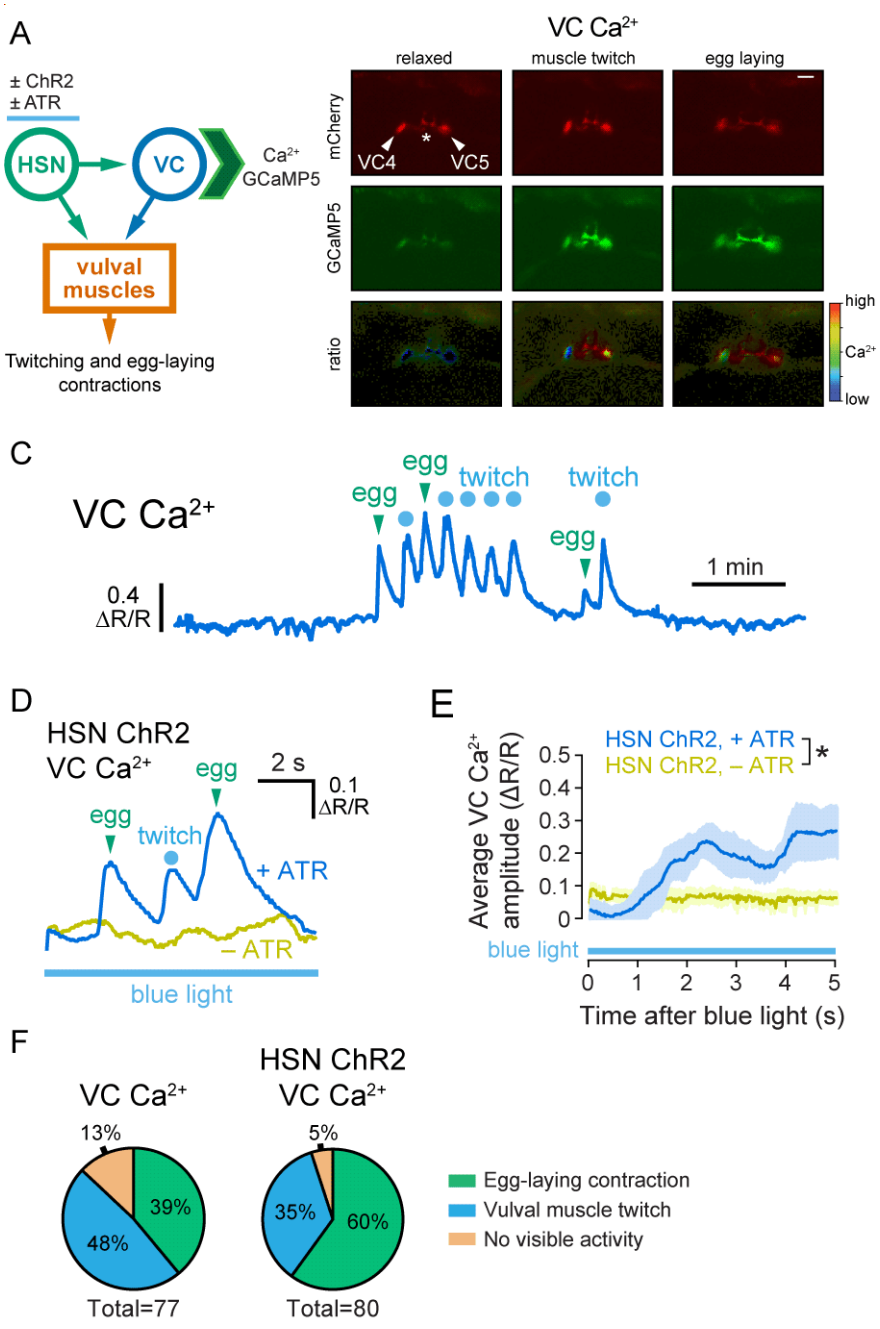

Figure 2. The VC neurons are active during both weak vulval muscle twitching and strong egg-laying contractions.

(**A**) Cartoon of circuit and experiments. GCaMP5 was expressed in the VC neurons to record Ca^{2+} activity, and Channelrhdopsin-2 was expressed in HSNs to provide optogenetic stimulation of egg laying. (**B**) Representative still images of VC mCherry, GCaMP5, and GCaMP5/mCherry ratio (ΔR/R) during inactive and active egg-laying behavior states. Asterisk indicates vulva. Scale bar is 20 μm. (**C**) Representative trace of VC GCaMP5/mCherry Ca^{2+} ratio in freely behaving, wild-type animals during an egg-laying active state. (**D**) Representative trace of VC GCaMP5/mCherry Ca^{2+} ratio after optogenetic stimulation of ChR2 in the HSN neurons in animals grown in the absence (-ATR, top) and presence (+ATR, bottom) during 10 s of continuous blue light exposure. (**E**) Average vulval muscle Ca^{2+} levels (mean ±95%

confidence intervals from 10 animals; asterisk indicates $p<0.0001$, Student's t test). (**F**) Graph showing vulval muscle contractile activity for each VC Ca^{2+} transient during endogenous egg-laying active states (left) or in response to HSN optogenetic stimulation (right).

The VC neurons promote vulval muscle activity and contraction

The VC motor neurons synapse onto the vulval and body muscles where they are thought to release acetylcholine to drive contraction (Duerr et al., 2008; White et al., 1986; Zhang et al., 2008). While VC activity and neurotransmission is not required for egg laying (Figure 1G and 1K; Laura E. Waggoner et al., 1998), the VCs may still release ACh to regulate vulval muscle contractility. To test if the VCs can excite the vulval muscles directly, we expressed Channelrhodopsin-2 in the VC neurons and performed ratiometric Ca^{2+} imaging in the vulval muscles after exposure to blue light (Figure 3A; Movie 3). Optogenetic stimulation of the VCs led to an acute induction of vulval muscle Ca^{2+} activity within 5 s but was unable to drive full vulval muscle contractions and egg release (Figure 3B and 3C). However, average vulval muscle Ca^{2+} transient amplitude after optogenetic stimulation was not significantly higher through the duration of the recording (Figure 3D). Vulval muscle Ca^{2+} transient frequency was reduced, which may result from the increased duration of each individual transient (Figures 3E and 3F). This result shows that VC activity alone is not able to maximally excite the vulval muscles to the point of egg laying, but that VC activity is excitatory and can sustain ongoing vulval muscle Ca^{2+} activity. We find these results consistent with a model where serotonin and NLP-3 neuropeptides released from HSN signal to enhance the excitability and contractility of the vulval muscles for egg laying while the ACh released from the VCs prolong the contractile phase to facilitate egg release.

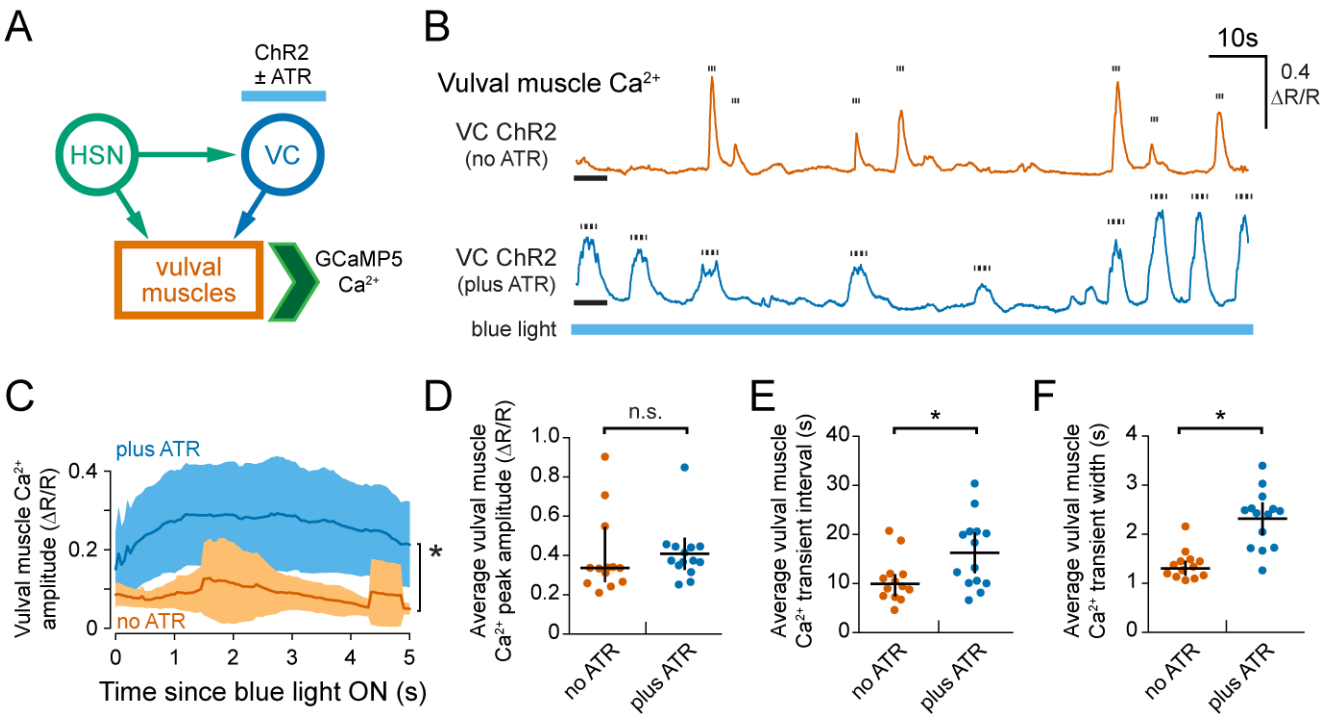

Figure 3. Optogenetic VC activation induces and sustains vulval muscle Ca^{2+} activity.

(**A**) Cartoon of circuit and experiment. Channelrhdopsin-2 was expressed in the VC neurons and GCaMP5 was expressed in the vulval muscles. (**B**) Representative traces of vulval muscle GCaMP5/mCherry Ca^{2+} ratio (ΔR/R) in animals grown in the absence (-ATR, top) or presence (+ATR, bottom) in response to 5 minutes of continuous blue light exposure. Tick marks show duration at half-maximal amplitude of each measured Ca^{2+} transient. Black bar indicates first 5 seconds following blue light exposure. (**C**) Averaged vulval muscle Ca^{2+} transient activity (shaded region indicates ±95% confidence intervals) during the first 5 seconds of optogenetic activation of the VC neurons in -ATR (control; blue) and +ATR conditions (orange; asterisk indicates p=0.003, Student's t test; n≥13 animals). (**D**) Scatterplot showing the average peak amplitude of vulval muscle Ca^{2+} transients (±95% confidence intervals) per animal in response to VC optogenetic stimulation during 5 minutes of continuous blue light (n.s. indicates p>0.05; Student's t test). (**E**) Scatterplot showing the average time between vulval muscle Ca^{2+} transients (±95% confidence intervals) per animal during VC optogenetic stimulation during 5 minutes of continuous blue light (asterisk indicates p=0.0236, Student's t test). (**F**) Scatterplot showing the average vulval muscle Ca^{2+} transient width (±95% confidence intervals) per animal during VC optogenetic stimulation during 5 minutes of continuous blue light (asterisk indicates p<0.0001, Student's t test; error bars indicate 95% confidence intervals for the mean).

The VCs facilitate successful vulval opening during egg laying

Loss of VC activity or synaptic transmission caused a specific defect in serotonin-induced egg laying, suggesting the VCs are required for proper vulval muscle Ca^{2+} activity and/or

contractility. We recorded vulval muscle Ca^{2+} activity in freely behaving animals transgenically expressing Tetanus Toxin in the VCs (Figure 4A; Movie 4). Vulval muscle Ca^{2+} activity in wild-type animals is characterized by low activity during the ~20 minute egg-laying inactive state, and periods of high activity during the ~2 minute egg-laying active state (Figure 4B; Collins et al., 2016; Laura E. Waggoner et al., 1998). Expression of Tetanus Toxin in the VCs did not significantly affect the overall frequency or amplitude of vulval muscle Ca^{2+} transients during egg-laying inactive states compared to wild-type control animals (Figures 4C and 4D). However, inhibition of VC neurotransmission led to larger amplitude Ca^{2+} transients during the active phase (Figure 4D). Since previous work suggested the VCs release ACh that inhibits egg laying (Bany et al., 2003), the simplest explanation for this phenotype would be that the VCs normally inhibit vulval muscle Ca^{2+} activity. However, our results show optogenetic activation of the VCs increased vulval muscle Ca^{2+} transient duration with minimal effect on amplitude (Figures 3C, 3D, and 3F). Further inspection of vulval muscle Ca^{2+} traces of individual animals showed that transgenically expressing Tetanus Toxin in the VCs had large vulval muscle Ca^{2+} transients of amplitude similar to egg-laying Ca^{2+} transients (>1.0 $\Delta R/R$), but without an egg being successfully released (Figure 4B and 4E; Movie 4). We termed these “failed egg-laying events.” Such failed egg-laying events were infrequent in vulval muscle Ca^{2+} recordings from wild-type animals, but they occurred more frequently than successful egg-laying events in transgenic animals expressing Tetanus Toxin in the VCs (Figure 4E). Based on these results, it appears that VC neurotransmission does not initiate vulval muscle Ca^{2+} transients but is instead critical for coordinating vulval muscle Ca^{2+} activity and contraction across the vulval muscle cells to allow for successful egg release.

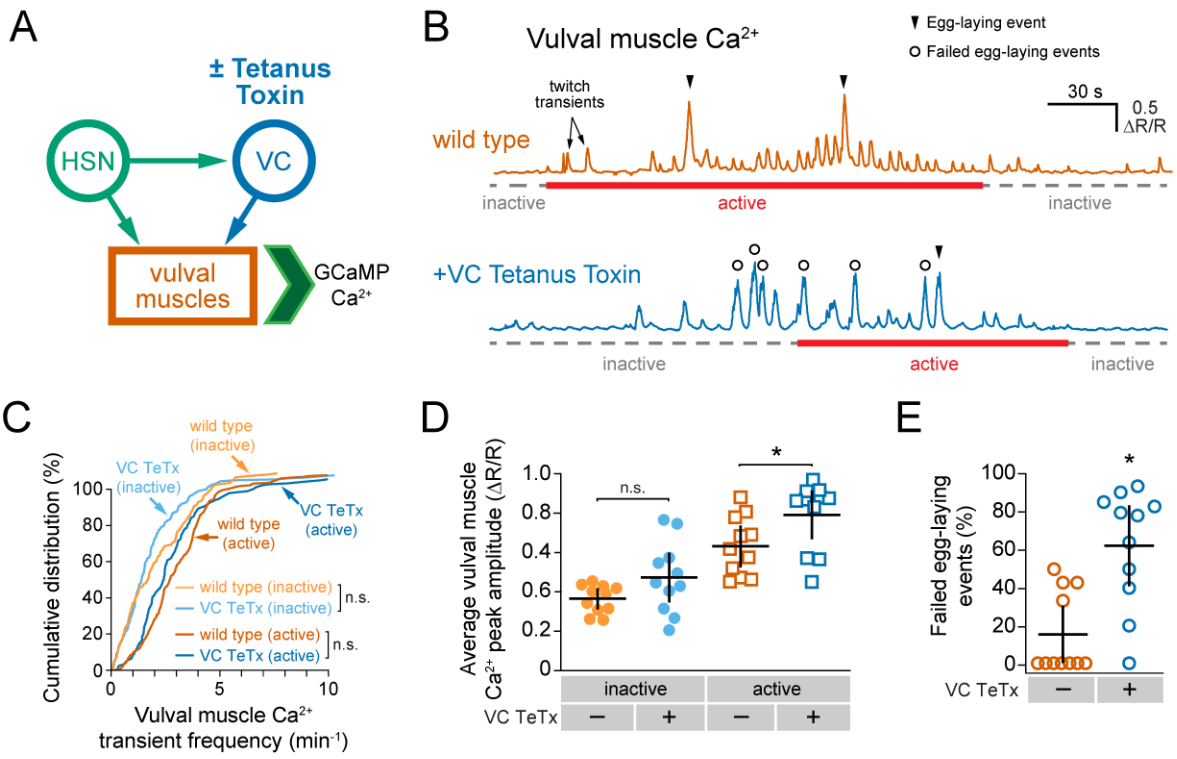

Figure 4. Blocking VC neurotransmission reduces the success rate of egg laying.

(**A**) Cartoon of circuit and experiment. Tetanus Toxin (TeTx) was expressed in the VC neurons to block their neurotransmitter release and GCaMP5 was expressed in the vulval muscles to record Ca^{2+} activity. (**B**) Representative traces of vulval muscle GCaMP5/mCherry Ca^{2+} ratio (ΔR/R) in wild-type (top) and Tetanus Toxin expressing transgenic animals (bottom). Arrowheads indicate successful egg-laying events, and open circles indicate strong (>1.0 ΔR/R) vulval muscle Ca^{2+} transients of "failed egg-laying events." Egg-laying behavior state (inactive or active) duration is indicated below each trace. (**C**) Cumulative distribution plots of all vulval muscle Ca^{2+} transients across wild-type and transgenic animals expressing TeTx in the VCs. Transients were parsed into egg-laying active and inactive phases (n.s. indicates $p>0.05$, Kruskal-Wallis test with Dunn's correction for multiple comparisons). (**D**) Average vulval muscle Ca^{2+} transient peak amplitudes per animal during the inactive and active egg-laying phase (asterisk indicates $p=0.0336$, one-way ANOVA with Bonferroni's correction for multiple comparisons). (**E**) Percentage of failed egg-laying events in wild-type and transgenic animals expressing TeTx in the VCs (asterisk indicates $p=0.0014$, Mann-Whitney test; n=11 animals per genotype).

Egg laying is a two-step process where strong vulval muscle Ca^{2+} activity drives the synchronous contraction of all vulval muscle cells across both the anterior and posterior halves (Brewer et al., 2019; Li et al., 2013) that allows for the mechanical opening of the vulva in phase

with locomotion for efficient egg release (Collins et al., 2016; Collins & Koelle, 2013). Egg-laying events are characterized by coordinated Ca^{2+} activity between the vm1-type vulval muscles that extend to the ventral tips of the vulva and the medial vm2-type vulval muscles that lead to contraction (Figure 5A). This Ca^{2+} activity is distinct from weak vulval muscle twitching contractions that are confined to the vm1 muscles (Figure 5A; Collins & Koelle, 2013). To understand why egg laying was less likely to occur during strong vulval muscle Ca^{2+} transients in VC-silenced animals, we measured features of contractile events during egg laying. Contraction can be directly quantified by measuring the reduction in muscle area in fluorescent micrographs, and vulval opening can be quantified by measuring the changing distance between the anterior and posterior muscle halves (Figure 5A). During egg-laying events in wild-type animals, a strong cytosolic Ca^{2+} transient drives a ~50 μm^2 contraction of muscle size followed by a rebound phase after egg release (Figure 5B, top and middle). Simultaneously, the anterior and posterior muscles separate by ~10 µm, facilitating egg release (Figure 5B, bottom). We found few differences in the kinetics or extent of vulval muscle opening between wild-type and Tetanus Toxin-expressing transgenic animals during successful egg-laying events (compare Figures 5B and 5C). The vulval muscles opened wider and the degree of contraction was greater during egg-laying events in animals where VC transmission was silenced with Tetanus Toxin (Figure 5C), possibly because the vulval muscle Ca^{2+} rise started earlier in these animals. During failed egg-laying events, the vulval muscles showed only modest contraction and only separated by ~5 µm, insufficient to allow egg release, despite reaching similar levels of cytosolic Ca^{2+} (Figure 5D). This failure to open the vulva was more pronounced in animals where VC transmission was blocked by Tetanus Toxin (compare Figures 5D and 5E). In contrast, animals with silenced VC transmission have many more failed egg-laying events and exhibit vulval opening kinetics more similar to twitches (Figure 5F). To understand the relationship between vulval muscle Ca^{2+} levels and vulval opening, we measured the distance between anterior and

posterior vulval muscles during weak twitching, failed egg-laying events, and successful egg-laying events (Figure 5F). In both wild-type and Tetanus Toxin-expressing animals, we noted a linear relationship of low but positive slope between vulval opening and Ca^{2+} levels <1.0 ΔR/R (Δopening / ΔCa^{2+}) during weak twitching contractions (Figure 5F and 5G). However, as Ca^{2+} levels rose above 1.0 ΔR/R, the muscles reached threshold for full opening, allowing successful egg release (Figure 5F). The steep, linear Δopening / ΔCa^{2+} relationship during failed egg-laying events suggests a threshold of Ca^{2+} drives an all-or-none transition to full contraction, vulval opening, and egg release. In VC-silenced animals, the shallow Δopening / ΔCa^{2+} relationship continued as weak twitches transitioned into failed egg-laying events, with many strong vulval muscle Ca^{2+} transients failing to open the vulva sufficiently for egg release (Figure 5G). However, successful egg-laying events in VC-silenced animals still showed a sharp threshold between Ca^{2+} levels and the degree of vulval opening. This raises the possibility of two types of failed egg-laying events: one that is shared with wild-type animals, and another that is unique to VC-silenced animals.

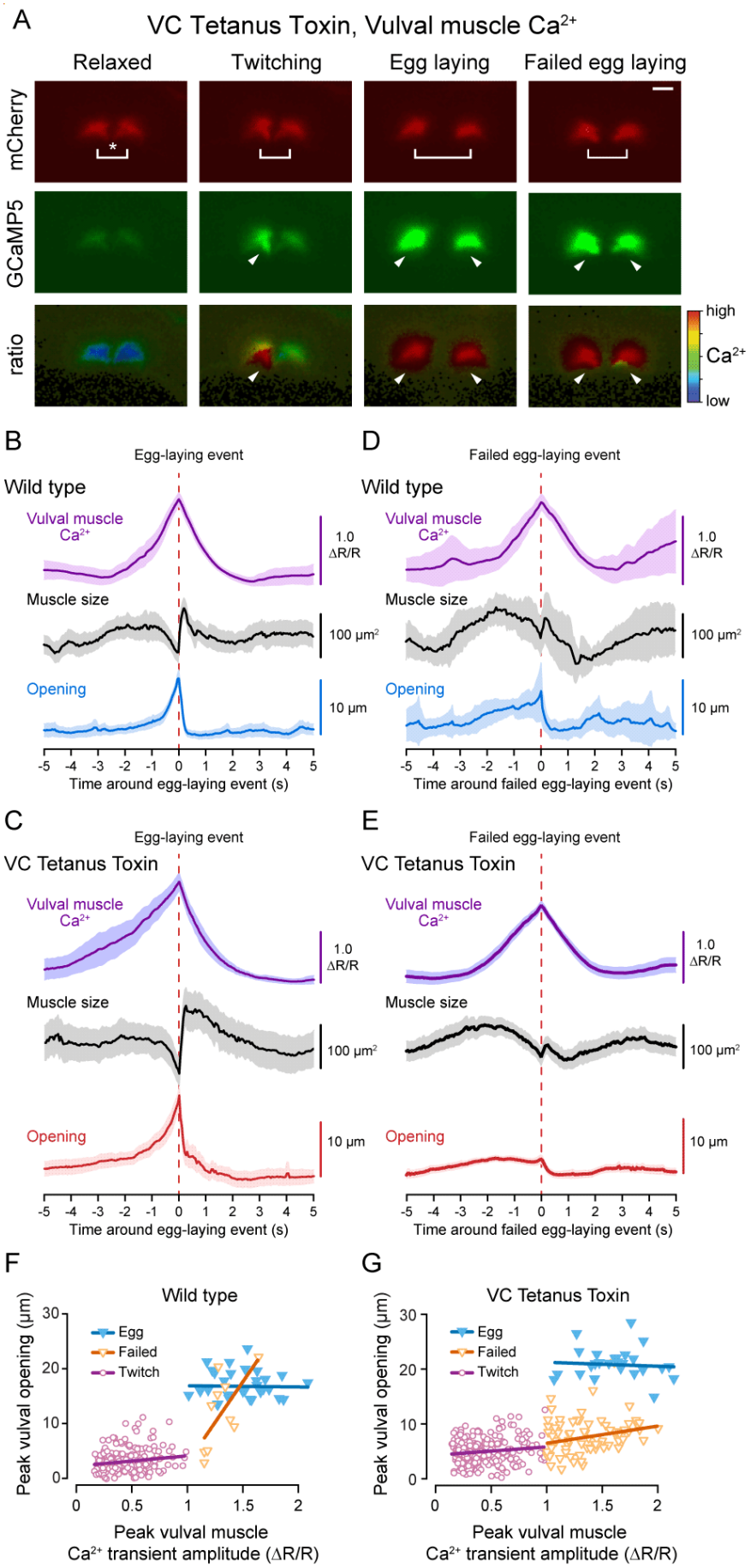

Figure 5: Blocking VC neurotransmission decouples vulval muscle Ca^{2+} activity and egg laying.

(**A**) Vulval muscle sizes and distances were quantified by measuring the changes in area and centroid of the anterior and posterior muscle groups in mCherry channel micrographs during GCaMP5/mCherry ratiometric imaging. Shown are still images of the vulval muscles during representative muscle states of relaxation, twitching, egg laying, and failed egg-laying events. Brackets indicate the distance between the centroid of vulval muscle halves, arrowheads indicate high Ca^{2+} activity, and asterisk indicates vulva. Scale bar is 20 µm. (**B-D)** Mean traces (±95 confidence intervals) of vulval muscle Ca^{2+} (GCaMP5/mCherry ratio), vulval muscle area (μm^2), and vulval muscle centroid distance (µm) during successful (B and C) and failed egg-laying events (D and E) in wild-type (B and D) and transgenic animals expressing Tetanus Toxin in the VC neurons (C and E). (**E-F**) Scatter plot showing peak vulval muscle Ca^{2+} amplitude in relation to the corresponding vulval muscle opening distance in wild-type (E) and transgenic animals expressing Tetanus Toxin in the VC neurons (F). Lines through points represent simple linear regression for each labeled grouping.

VC neurotransmission regulates HSN command neuron and egg-laying circuit activity

The VC motor neurons have a number of synaptic partners, such as the vulval muscles, various locomotion motor neurons, and the HSN neurons (White et al., 1986). The HSN neurons are particularly interesting due to them being critical for egg-laying behavior and sharing significant sites of cross-innervation with the VCs (Schafer, 2006; White et al., 1986). The VC neurons have been suggested to release ACh which signals to inhibit egg-laying behavior via muscarinic GAR-2 receptors on the HSN neurons (Bany et al., 2003; Zhang et al., 2008). The HSNs variably express two muscarinic acetylcholine receptors, GAR-1 and GAR-2 (Fernandez et al., 2020). To determine whether VC synaptic transmission regulates egg laying via HSN, we recorded HSN Ca^{2+} activity in wild-type and transgenic animals expressing Tetanus Toxin in the VCs (Figure 6A). We observed a significant increase in HSN Ca^{2+} transient frequency when VC synaptic transmission was blocked compared to non-transgenic control animals (Figure 6B). We have previously shown that vulval muscle Ca^{2+} activity produces a retrograde signal that sustains

371 burst firing in the presynaptic HSNs, which could be mediated by the VC neurons (Ravi, Garcia,
372 et al., 2018). Such HSN burst firing during egg-laying active states is not driven by successful
373 egg-laying events but is enhanced by egg accumulation and feedback of vulval muscle Ca^{2+}
374 activity (Ravi, Garcia, et al., 2018). We found that animals where VC synaptic transmission was
375 blocked with Tetanus Toxin showed increased burst firing in HSN. While wild-type animals spent
376 ~11% of their time showing high frequency activity in the HSN neurons, transgenic animals
377 expressing Tetanus Toxin in the VC neurons spent ~21% showing high frequency burst firing
378 Ca^{2+} transients in the HSN neurons (Figure 6D). Because burst firing was increased in VC
379 Tetanus Toxin transgenic animals, synaptic transmission from the VCs does not mediate the
380 retrograde signal between the HSN neurons and vulval muscles. Once again, the simplest
381 explanation for these results would be that VC neurotransmission is instead inhibitory toward the
382 HSNs such as proposed in previous studies (Bany et al., 2003; Zhang et al., 2008), but the
383 steady-state egg accumulation of animals expressing VC-specific Tetanus Toxin or HisCl is
384 normal (Figure 1G, K). Because VC Tetanus Toxin expressing animals also have more frequent
385 failed egg-laying events (Figure 5E), we propose that the increased HSN burst firing we see in
386 VC Tetanus Toxin transgenic animals results from the egg-laying circuit entering into and staying
387 in the active state until it receives feedback of successful egg release, not just feedback of
388 ongoing vulval muscle Ca^{2+} activity.
389

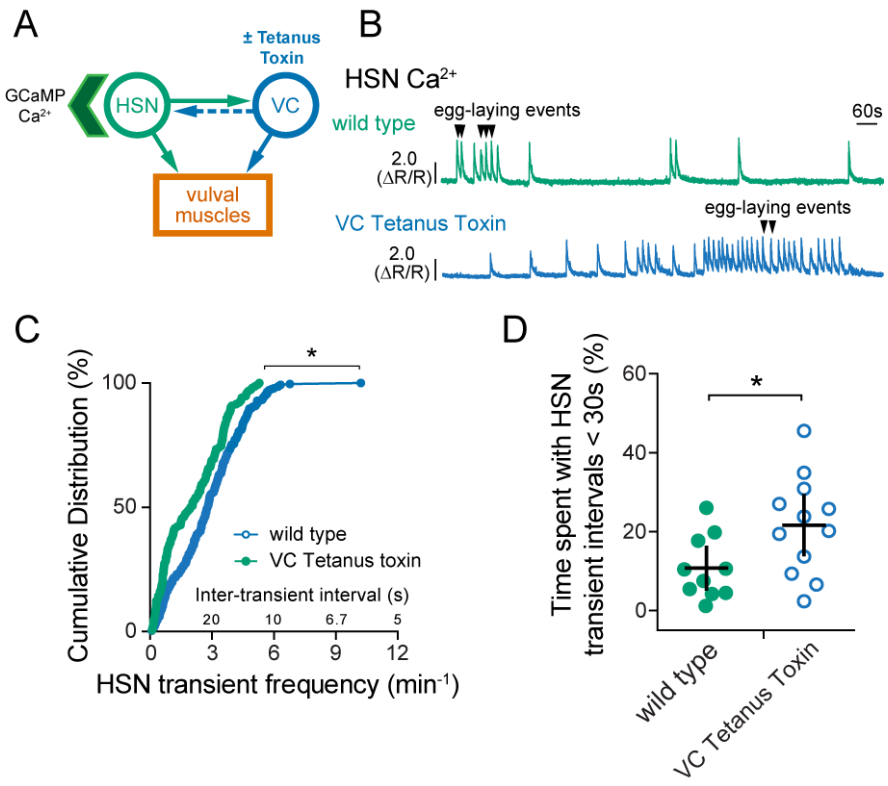

Figure 6. Blocking VC neurotransmission increases HSN Ca^{2+} activity.

(**A**) Cartoon of circuit and the experiment. Tetanus Toxin (TeTx) was expressed in the VC neurons to block their neurotransmitter release and HSN Ca^{2+} activity was recorded through GCaMP5 imaging. (**B**) Representative traces of HSN neuron GCaMP5/mCherry Ca^{2+} ratio ($\Delta R/R$) in a wild-type background (top, green) and animals expressing Tetanus Toxin in the VCs (bottom, blue). (**C**) Cumulative distribution plots of the instantaneous frequency of HSN Ca^{2+} transients in wild-type and Tetanus Toxin-expressing animals (asterisk indicates p=0.0006, Kolmogorov-Smirnov test). (**D**) Scatter plot for the percentage of time each animal spent with HSN Ca^{2+} inter-transient intervals that were less than 30 seconds, an indicator of hyperactivity (asterisk indicates *p*=0.00272, Student's test; error bars indicate 95% confidence intervals for the mean).

The VC motor neurons are responsive to vulval muscle activity and contraction

VC Ca^{2+} activity is coincident with strong vulval muscle twitching and egg-laying contractions (Figure 2; Collins et al., 2016). In addition to making synapses onto the vm2 muscles whose contraction drives egg laying, the VCs extend neurites along the vulval hypodermis devoid of synapses (White et al., 1986), suggesting the VCs may respond to vulval

opening. To test this model, we sought to induce vulval opening independent of endogenous circuit activity and presynaptic input from the HSNs. We transgenically expressed Channelrhodopsin-2 specifically in the vulval muscles using the *ceh-24* promoter to stimulate the vulval muscles and used GCaMP5 to record blue-light induced changes in vulval muscle Ca^{2+} activity (Figure 7A and Movie 5). Optogenetic stimulation of the vulval muscles triggered an immediate rise in vulval muscle cytosolic Ca^{2+}, tonic contraction of the vulval muscles, vulval opening, and egg release (Figures 7B and 7C). Even though optogenetic stimulation resulted in sustained vulval muscle Ca^{2+} activity and contraction, vulval opening and egg release remained rhythmic and phased with locomotion, as previously observed in wild-type animals (Collins et al., 2016; Collins & Koelle, 2013). Simultaneous bright field recordings showed the vulva only opened for egg release when the adjacent ventral body wall muscles were in a relaxed phase (Movie 6). We have previously shown that eggs are preferentially released when the vulva is at a particular phase of the body bend, typically as the ventral body wall muscles anterior to the vulva go into a more relaxed state (Collins et al., 2016; Collins & Koelle, 2013). We now interpret this phasing of egg release with locomotion as evidence that vulval muscle Ca^{2+} activity drives contraction, but the vulva only opens for successful egg release when contraction is initiated during relaxation of the adjacent body wall muscles. Together, these results show that optogenetic stimulation of the vulval muscles is sufficient to induce vulval muscle Ca^{2+} activity and contraction for egg release.

To test the hypothesis that the VCs respond to vulval muscle activation, we recorded changes in VC Ca^{2+} upon optogenetic stimulation of the vulval muscles (Figure 7D). We observed a robust induction of VC Ca^{2+} activity upon blue light illumination (Figures 7E and 7F). The rise in VC Ca^{2+} occurred before the first egg-laying event, suggesting that this process is dependent on muscle activity and not necessarily the passage of an egg (Figure 7G; Movie 7).

This result demonstrates that the VCs can become excited in response to activity of the postsynaptic vulval muscles. What is the mechanism for VC activation by the vulval muscles? The VCs make both chemical and electrical synapses on vulval muscles (Cook et al., 2019; White et al., 1986). Depolarization of the vulval muscles might be expected to electrically propagate to the VC and trigger an increase in VC Ca^{2+} activity. Another possibility is that the VCs are mechanically activated in response to vulval muscle contraction and/or vulval opening. To test these alternate models, we optogenetically stimulated the vulval muscles of *unc-54* muscle myosin mutants, which are unable to contract their muscles, and recorded VC Ca^{2+} activity (Figure 7D; Movie 8). We found optogenetic activation of the vulval muscles failed to induce VC Ca^{2+} activity in *unc-54* mutants compared to the wild-type background (Figures 7G and 7H). While *unc-54* mutants appear to show some increase in VC Ca^{2+} activity following blue light stimulation of the vulval muscles, this increase was not statistically significant, suggesting indirect excitation of the VCs through gap junctions is insufficient on its own to induce robust VC Ca^{2+} activity. Together, these results support a model where the VC neurons are mechanically activated in response to vulval muscle contraction. Mechanical activation appears to drive VC activity and is mediated through the VC4 and VC5 neurites which are most proximal to the vm2 vulval muscles and vulval canal through which eggs are laid. Following this mechanical activation step, excitation of vulva-proximal VCs may lead to the cross-stimulation of the more distal VC neurons to coordinate locomotion and body posture during egg-laying behavior.

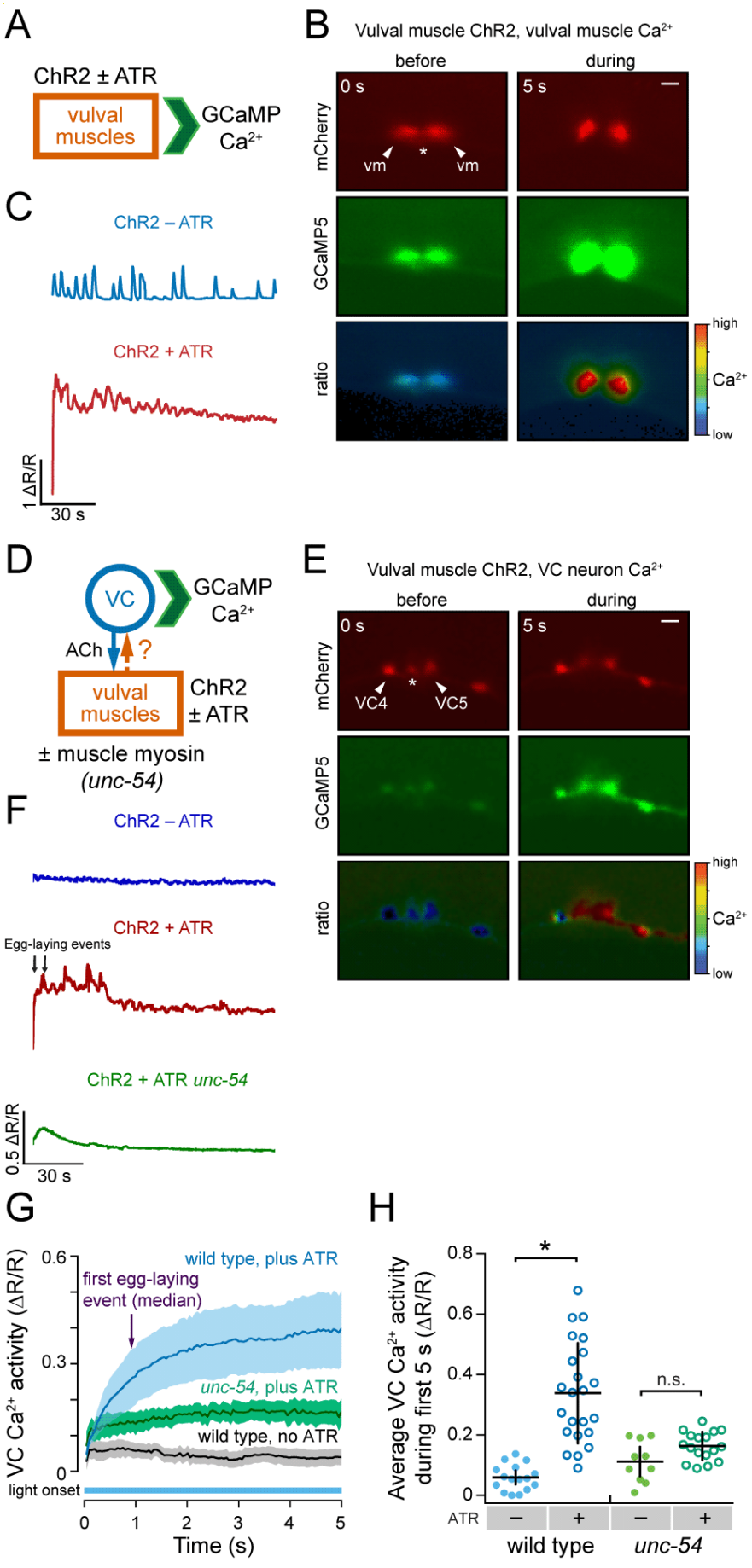

Figure 7. Optogenetic activation and contraction of the vulval muscles drives VC neuron activity.

(**A**) Cartoon of experiment. Channelrhodopsin-2 and GCaMP5 were expressed in the vulval muscles to monitor cytosolic Ca^{2+} after optogenetic stimulation. (**B**) Representative still images of vulval muscle mCherry, GCaMP5, and GCaMP5/mCherry ratio during optogenetic activation of the vulval muscles. Arrowheads indicate each vulval muscle half, and asterisk indicates vulva. Scale bar is 20 μm. (**C**) Representative traces of vulval muscle GCaMP5/mCherry Ca^{2+} ratio (ΔR/R) in animals expressing ChR2 in the vulval muscles in the absence (-ATR , top) or presence (+ATR, bottom) of all-*trans* retinal during 3 minutes of continuous blue light exposure. (**D**) Cartoon of circuit and experiment. Channelrhdopsin-2 was expressed in the vulval muscles and GCaMP5 was expressed in the VC neurons to record Ca^{2+} activity in wild-type or *unc-54* myosin null mutant animals. (**E)** Representative still images of VC neuron mCherry, GCaMP5, and GCaMP5/mCherry ratio during optogenetic activation of the vulval muscles. Arrowheads indicate VC neuron cell bodies, and asterisk indicates vulva. Scale bar is 20 μm. (**F**) Representative traces of VC neuron GCaMP5/mCherry Ca^{2+} ratio (ΔR/R) in animals expressing ChR2 in the vulval muscles in the absence (-ATR , top) or presence (+ATR, bottom) of all-*trans* retinal during 3 minutes of continuous blue light exposure. **(G)** Averaged VC Ca^{2+} responses during the first 5 s. Error bands represent ±95 confidence intervals for the mean. (**H)** Scatter plot showing the average VC Ca^{2+} response during the first 5 seconds of optogenetic stimulation of the vulval muscles. Asterisk indicates $p<0.0001$; n.s. indicates $p>0.05$ (one-way ANOVA with Bonferroni's correction for multiple comparisons).

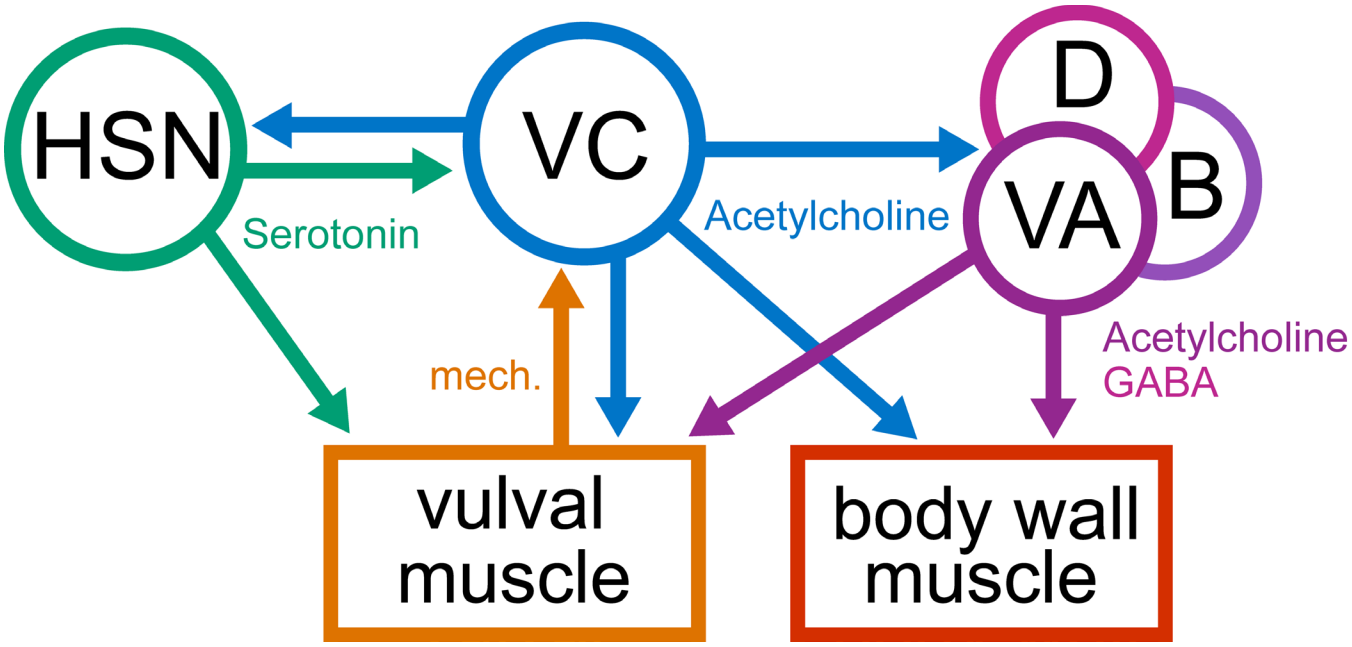

Figure 8. The VC neurons function to coordinate synchronized contraction of the vulval muscles for egg laying in response to serotonin-mediated potentiation.

Discussion

The connectome of *C. elegans* has greatly informed neural circuit studies and has revealed that connectivity alone is not sufficient to explain nervous system operations (Bargmann, 2012; Bentley et al., 2016). In the present study, we examined the neural circuit driving egg-laying behavior in *C. elegans* at a cellular resolution to reveal functional pathways and elements of the behavior that had not been discernable through connectome or prior genetic studies (Figure 8). We show that serotonin promotes egg laying in a way that requires the hermaphrodite-specific, cholinergic VC motoneurons. The hermaphrodite-specific HSN command neurons have previously been shown to be the primary source of serotonin within the egg-laying circuit and make synapses onto both the VCs and vulval muscles (Cook et al., 2019; Waggoner et al., 1998; White et al., 1986). Our data shows that HSN activity acts to excite the vulval muscles and VCs, and that VC Ca^{2+} activity is closely associated with visible vulval muscle contraction. In the

493 absence of HSN-mediated potentiation, the VCs are able to excite the vulval muscles, but not to
494 the threshold required for egg laying. This sub-threshold interaction is consistent with a model
495 where serotonin-mediated potentiation of the VCs and/or vulval muscles is required before the
496 VCs can facilitate egg laying through timely excitatory input. In the absence of VC
497 neurotransmission, the HSN command neurons and the vulval muscles show excess Ca^{2+}
498 activity, but this excess activity does not correspond to increased egg laying. Instead, we find
499 that the vulval muscles are less efficient at opening the vulva, indicating the VCs have a role in
500 facilitating vulval muscle contraction. We thus interpret the excess HSN and vulval muscle
501 activity as a natural consequence of egg-laying circuit activity without feedback of successful
502 egg release (Collins et al., 2016). Surprisingly, optogenetic activation and contraction of the
503 postsynaptic vulval muscles is sufficient to drive presynaptic VC Ca^{2+} activity. We propose that
504 serotonin released from the HSNs signals to promote both vulval muscle contractility and VC
505 sensitivity to that contraction. Following this potentiation, vulval muscle twitch contractions are
506 able to mechanically activate the VCs to release excitatory acetylcholine as part of a positive-
507 feedback loop until the vulval muscles are fully contracted and egg laying occurs.

508 The physiological basis for the distinction between vulval muscle twitching, egg-laying
509 events, and failed egg-laying events may result from different presynaptic inputs (Collins &
510 Koelle, 2013; Cook et al., 2019; White et al., 1986). Twitching is limited to Ca^{2+} activity in the
511 vm1 vulval muscles and occurs at a similar phase of locomotion as egg laying (Collins & Koelle,
512 2013). The vm1 muscles receive synaptic input from single Ventral Type A and Type B (VA and
513 VB, respectively) motor neurons (Figure 8; Cook et al., 2019; White et al., 1986). The VA and
514 VB motor neurons are part of the locomotion circuit that drive forward and reverse locomotion,
515 respectively, suggesting they may signal to coordinate egg-laying and locomotion behaviors
516 (Collins et al., 2016; Hardaker et al., 2001; Zhen & Samuel, 2015). The vm2 vulval muscles

receive synaptic input from the HSN and VC neurons (Cook et al., 2019; White et al., 1986), and synaptic input from the HSNs onto the vm2 muscles helps coordinate anterior and posterior muscle contraction (Li et al., 2013). The VCs also regulate locomotion, potentially through the GABAergic motor neurons or via direct release of ACh that drives excitation and contraction of the body wall muscles to slow locomotion (Figure 8; Collins et al., 2016). Slowing of locomotion before egg laying may provide time for the vulval muscles to fully contract (Collins et al., 2016; Collins & Koelle, 2013). This slowing appears to hold the animal in a body posture that is favorable for vulval opening and egg release, which would be consistent with our finding that VC activity causes elongated vulval muscle Ca^{2+} twitch transients (Figure 3). In this role, the VCs would be signaling to the rest of the egg-laying circuit and locomotion circuit that the vulva is open so that body posture can be held in a favorable phase for egg release. Failed egg-laying events could occur because of disrupted phasing of the locomotion pattern with activity in the egg-laying circuit. Since twitches and egg-laying events occur at a specific phase of the locomotion pattern, the opening of the vulva and egg release may require not only coordinated muscle contraction, but also the relaxation of immediately proximal body wall muscles so that they cannot physically resist the opening of the vulva. Thus, the VCs may act in timing the excitation of the vm2 muscles in relation to excitatory input from the VA/VB locomotion motor neurons onto the vm1 muscles, facilitating full contraction and egg laying in phase with locomotion.

Why are the VCs required for serotonin-induced egg laying? Serotonin is released by the HSN command neurons along with NLP-3 neuropeptides to initiate the active phase of egg-laying behavior (Brewer et al., 2019; Collins et al., 2016; Shyn et al., 2003; Waggoner et al., 1998). Serotonin signals through several G-protein coupled receptors including the 5-HT_{1C} ortholog SER-1 and the 5-HT_7 ortholog SER-7 expressed on the vulval muscles (Hapiak et al.,

2009; Hobson et al., 2006; Xiao et al., 2006). These serotonin receptors are thought to act through $G\alpha_q$ and $G\alpha_s$ signaling pathways, respectively, which activate EGL-19 L-type voltage-gated Ca^{2+} channels in the vulval muscles to enhance their response to other excitatory input (Schafer, 2006; Waggoner et al., 1998; Zhang et al., 2008). Serotonin acting through SER-7 has previously been shown to initiate neural circuit activity, such as in feeding behavior (Song et al., 2013). SER-7 is also expressed in the VC neurons (Fernandez et al., 2020), and serotonin stimulates VC Ca^{2+} activity (Zhang et al., 2008). Similar to animals where VC neurotransmitter release is blocked, *ser-7* mutants also fail to respond to exogenous serotonin (Hobson et al., 2006). Targets of serotonin within the VCs may include N/P/Q-type Ca^{2+} channels such as UNC-2 which promote neurotransmitter release (Schafer et al., 1996). Following serotonergic potentiation, the VCs may be close enough to threshold to become mechanically excited in response to vm1-mediated vulval muscle twitches, leading to excitatory neurotransmitter release onto the vm2 vulval muscles to drive complete vulval muscle contraction for egg release.

Many behaviors require retrograde feedback to help fine-tune movements and make adjustments based on the changing internal and external environment, such as with wing-beat patterns in *Drosophila* or head-eye coordination in humans (Bartussek & Lehmann, 2016; Fang et al., 2015). We find that the downstream target of the egg-laying neural circuit, the vulval muscles, signals upstream to facilitate proper completion of the behavior. We postulate that such retrograde signaling is critical for two reasons. First, it can act to feedback inhibit the circuit to signal when the behavior has been executed. We find that vulval muscle contraction activates the VCs, which may inhibit the egg-laying circuit through release of acetylcholine acting on metabotropic receptors such as GAR-2 on the HSNs, vulval muscles, and uv1 cells (Bany et al., 2003; Fernandez et al., 2020; Zhang et al., 2008, 2010). GAR-2 has been shown to act in parallel with ionotropic receptors to differentially modulate locomotion behavior, providing both short-

565 and longer-term effects in response to cholinergic signaling (Dittman & Kaplan, 2008). Second,
566 retrograde signaling can create a feed-forward excitation to facilitate full execution of a behavior.
567 In this circuit model, HSN command neuron signaling potentiates the excitatory VCs to help
568 ensure vulval muscle twitches are converted into full egg-laying contractions. This type of feed-
569 forward activity has been demonstrated in the SMDD neurons in which the TRPC channels,
570 TRP-1 and TRP-2, are mechanically activated by neck muscle contractions to influence neck
571 steering behavior (Yeon et al., 2018). How the VC neurons are mechanically activated is still
572 unclear, but the VCs do express innexin gap junction proteins (Altun et al., 2009) that have
573 recently been shown to respond to mechanical activation as hemichannels (Walker & Schafer,
574 2020).

575 In all, the VC neurons and the egg-laying circuit present a unique model system for
576 investigating how different forms of feedback work together to drive a robust behavior. The
577 elucidation of the cellular and molecular mechanisms underlying these distinct forms of feedback
578 could help the understanding of human neurological diseases where muscle coordination and
579 proprioception are dysregulated, such as in Parkinson's and Huntington disease (Bargmann,
580 2012; Lukos et al., 2013).
581

Movie 1. GCaMP5/mCherry ratio recording of VC Ca^{2+} activity during the egg-laying active state.

Ratio of GCaMP5 and mCherry fluorescence in the VC neurons mapped onto a false color spectrum ranging from blue (low Ca^{2+}) to red (high Ca^{2+}). The VC neurons show high Ca^{2+} activity and physical displacement as the vulval muscles contract and an egg passes through the vulva to be laid. The Ca^{2+} activity then returns to a low level until a vulval muscle twitch occurs (0:09) followed by another egg-laying event.

Movie 2. GCaMP5/mCherry ratio recording of VC Ca^{2+} activity in response to optogenetic stimulation of the HSNs.

Ratio of GCaMP5 and mCherry fluorescence in the VC neurons mapped onto a false color spectrum ranging from blue (low Ca^{2+}) to red (high Ca^{2+}). Optogenetic activation of the HSN neurons initiates an egg-laying active state, which results in high VC Ca^{2+} transients (red), vulval muscle twitches, and egg laying. The VC Ca^{2+} returns to low activity (blue) in between twitch and egg-laying instances.

Movie 3. GCaMP5/mCherry ratio recording of vulval muscle Ca^{2+} in response to optogenetic stimulation of the VCs.

Ratio of GCaMP5 and mCherry fluorescence in the vulval muscles mapped onto a false color spectrum ranging from blue (low Ca^{2+}) to red (high Ca^{2+}). Optogenetic activation of the VC neurons induces vulval muscle Ca^{2+} activity and twitches, but not egg laying.

Movie 4. GCaMP5/mCherry ratio recording of vulval muscle Ca^{2+} during the egg-laying active state when synaptic transmission from the VC neurons is blocked by Tetanus Toxin.

Ratio of GCaMP5 and mCherry fluorescence in the vulval muscles mapped onto a false color spectrum ranging from blue (low Ca^{2+}) to red (high Ca^{2+}). The vulval muscles still exhibit twitches and egg-laying events but will also frequently fail to lay eggs in response to high Ca^{2+} activity, termed “failed egg-laying events”.

Movie 5. GCaMP5/mCherry ratio recording of vulval muscle Ca^{2+} in response to optogenetic stimulation of the vulval muscles.

Ratio of GCaMP5 and mCherry fluorescence in the vulval muscles mapped onto a false color spectrum ranging from blue (low Ca^{2+}) to red (high Ca^{2+}). Optogenetic activation of the vulval muscles induces immediate and sustained vulval muscle contraction, high Ca^{2+} activity, and periodic egg-laying events.

Movie 6. Brightfield recording of vulval opening and egg laying in response to optogenetic stimulation of the vulval muscles.

Brightfield recording of egg laying in response to optogenetic vulval muscle activation. Optogenetic activation of the vulval muscles induces tetanic vulval muscle contraction, but vulval opening and egg release remains phased with the body bends of locomotion.

Movie 7. GCaMP5/mCherry ratio recording of VC Ca^{2+} in response to optogenetic stimulation of the vulval muscles.

Ratio of GCaMP5 and mCherry fluorescence in the VCs mapped onto a false color spectrum ranging from blue (low) to red (high). Optogenetic activation of the vulval muscles causes an immediate induction of VC Ca^{2+} activity that remains at a high level for the duration of the stimulation.

Movie 8. GCaMP5/mCherry ratio recording of VC Ca^{2+} during optogenetic vulval muscle activation in an *unc-54* myosin mutant background.

Ratio of GCaMP5 and mCherry fluorescence in the VCs mapped onto a false color spectrum ranging from blue (low Ca^{2+}) to red (high Ca^{2+}). Optogenetic activation of the vulval muscles induces immediate but greatly diminished VC Ca^{2+} activity compared to otherwise wild-type animals.

Materials & Methods

Nematode culture and strains

All *C. elegans* strains were maintained at 20 °C on Nematode Growth Medium (NGM) agar plates seeded with OP50 *E. coli* as described (Brenner, 1974). All assays were conducted on age-matched adult hermaphrodites at 24-30 h past the late L4 stage, unless otherwise stated. A list of all strains generated and used in this study can be found in Table 1.

Plasmid and strain construction

Oligonucleotides were synthesized by IDT-DNA. PCR was performed using high-fidelity Phusion DNA polymerase (New England Biolabs) except for routine genotyping which was performed using standard Taq DNA polymerase. Plasmids were prepared using a Qiagen miniprep spin kit. DNA concentrations were determined using a Nano-Drop spectrophotometer.

Tetanus toxin (TeTx)-expressing transgenes:

VC neuron TeTx – A ~1.4 kB DNA fragment encoding Tetanus Toxin was cut from pAJ49 (Jose et al., 2007) with AgeI/XhoI, and ligated into a similarly digested pKMC145 [*lin-11::GFP::unc-54 3' UTR*] to generate pKMC282 [*lin-11::TeTx::unc-54 3' UTR*]. pKMC282 (50 ng/µl) was injected along with pL15EK (50 ng/µl; (Clark et al., 1994)) into LX1832 *lite-1(ce314) lin-15(n765ts) X* generating four independent transgenic lines of which one, MIA113 *keyEx32 [lin-11::TeTx::unc-54 3'UTR + lin-15(+)]; lite-1(ce314) lin-15(n765ts) X*, was used for integration. *keyEx32* was integrated with UV/TMP generating three independent integrants *keyIs32-33* and *keyIs46 [lin-11::TeTx::unc-54 3'UTR + lin-15(+)].* Each transgenic line was backcrossed six times to LX1832 generating strains MIA144-146. All transgenic strains appeared phenotypically similar, and

MIA144 and MIA146 were used for experiments and further crosses. To eliminate HSNs in animals lacking VC synaptic transmission, MIA26 *egl-1(n986dm) V* mutant animals were crossed with MIA146 to generate MIA173 *keyIs46; egl-1(n986dm) V*; *lite-1(ce314) lin-15(n765ts) X*.

Histamine-gated chloride channel (HisCl)-expressing transgenes:

VC neuron HisCl – The ~1.3 kB DNA fragment encoding *Drosophila* histamine-gated chloride channel HisCl1 was PCR amplified from pNP403 (Pokala et al., 2014) using the oligonucleotides 5'-GCG CCC GGG GTA GAA AAA ATG CAA AGC CCA ACT AGC AAA TTG G-3' and 5'-GCG GAG CTC TTA TCA TAG GAA CGT TGT CCA ATA GAC AAT A-3', cut with XmaI/SacI, and ligated into AgeI/SacI-digested pKMC145 to generate pAB2 [*lin-11::HisCl::unc-54 3'UTR]*. pAB2 (20 ng/µl) was injected into LX1832 along with pL15EK (50 ng/µl), generating the extrachromosomal line MIA93 *keyEx24 [lin-11::HisCl::unc-54 3'UTR + lin-15(+)]; lite-1(ce314) lin-15(n765ts) X*. The extrachromosomal transgene subsequently integrated using UV/TMP to generate the transgenes *keyIs23*-30 *[lin-11::HisCl::unc-54 3'UTR + lin-15(+)]*. Strains bearing these transgenes were then backcrossed to the LX1832 parent strain six times, generating strains MIA124, MIA125, MIA130, MIA131, and MIA132. All transgenic strains appeared phenotypically similar, and MIA125 was used for experiments and further crosses. To eliminate the HSN neurons in animals expressing HisCl in the VC neurons, MIA125 *keyIs23; lite-1(ce314) lin-15(n765ts) X* was crossed with MIA26 to generate MIA176 *keyIs23; egl-1(n986dm)*; *lite-1(ce314) lin-15(n765ts) X.*

Channelrhodopsin-2 (ChR2)-expressing transgenes:

686 Vulval muscle ChR2 – To express ChR2 in the vulval muscles, the ~1 kB DNA fragment
687 encoding for ChR2 was PCR amplified from pRK7 [*del-1::ChR2(H34R/T159C::unc-54 3' UTR]*
688 using oligonucleotides 5'-GCG GCT AGC ATG GAT TAT GGA GGC GCC CTG-3' and 5'-GCG
689 GGT ACC TCA GGT GGC CGC GGG GAC CGC GCC AGC CTC GGC C-3'. The amplicon and
690 recipient plasmid, pBR3 (Ravi, Garcia, et al., 2018), were digested with NheI/KpnI, generating
691 pRK11 [*ceh-24::ChR2(H34R/T159C)::unc-54 3' UTR*]. pRK11 (50 ng/µl) was injected into
692 LX1832 along with pL15EK (50 ng/µl) generating MIA212 *keyEx43* [*ceh-*
693 *24::ChR2(H34R/T159C)::unc-54 3'UTR + lin-15(+)]* which was subsequently integrated with
694 UV/TMP, generating five independent integrated transgenes *keyIs47-51*. Strains carrying these
695 integrated transgenes were then backcrossed to the LX1832 parent strain six times, generating
696 the strains MIA229-232 and MIA242. All transgenic strains were phenotypically similar, and
697 MIA229 was used for experiments and further crosses.

698 VC ChR2 – The allele *keyIs3* was used to express ChR2 in the VC neurons under a modified
699 *lin-11* promoter, as previously described (Collins et al., 2016).

700 HSN ChR2 – The allele *wzIs30* was used to express ChR2 in the HSN neurons under the *egl-6*
701 promoter, as previously described (Collins et al., 2016; Emtage et al., 2012).

702

703 *Calcium reporter transgenes*:

704 Vulval muscle GCaMP5 – Vulval muscle Ca^{2+} activity was visualized using the strain LX1918
705 which co-expresses GCaMP5 and mCherry in the vulval muscles from the *unc-103e* promoter
706 (Collins et al., 2016). To analyze vulval muscle Ca^{2+} activity in animals where VC synaptic
707 transmission was blocked with Tetanus Toxin, LX1918 was crossed with MIA144 to generate
708 MIA183 *keyIs33*; *vsIs164 lite-1(ce314) lin-15(n765ts) X*. To analyze vulval muscle Ca^{2+} activity

709 in animals where the VC neurons could be optogenetically activated by ChR2, LX1918 was
710 crossed with MIA3 (Collins et al., 2016), to generate MIA221 *keyIs3; vsIs164 lite-1(ce314) lin-*
711 *15(n765ts) X.* To analyze vulval muscle Ca^{2+} activity in animals where the vulval muscles could
712 be optogenetically activated by ChR2, LX1918 was crossed with MIA229 to generate MIA250
713 *keyIs49*; *vsIs164 lite-1(ce314) lin-15(n765ts) X*.

714 VC neuron GCaMP5 – VC neuron Ca^{2+} activity was visualized using the strain LX1960 which
715 co-expresses GCaMP5 and mCherry in the VC neurons (Collins et al., 2016). To visualize VC
716 activity during optogenetic stimulation of the HSNs, the strain LX1970 was used (Collins et al.,
717 2016). To visualize VC activity after optogenetic stimulation of the vulval muscles, LX1960 was
718 crossed with MIA229 to generate MIA241 *vsIs172*; *keyIs48 lite-1(ce314) lin-15(n765ts) X*. To
719 visualize VC activity after optogenetic stimulation of the vulval muscles when muscle contraction
720 is impaired, CB190 *unc-54(e190) I* myosin heavy chain null mutants were crossed with LX1832
721 to generate MIA274 *unc-54(e190) I*; *lite-1(ce314) lin-15(n765ts) X.* MIA274 was then crossed
722 with MIA241 to generate MIA298 *keyIs48; vsIs172; unc-54(e190) I; lite-1(ce314) lin-15(n765ts)*
723 *X*.

724 HSN neuron GCaMP5 – HSN neuron Ca^{2+} activity was visualized using the strain LX2004 which
725 co-expresses GCaMP5 and mCherry in the HSN neurons (Collins et al., 2016). To visualize HSN
726 Ca^{2+} after neurotransmission from the VC neurons is blocked by Tetanus Toxin, LX2004 was
727 crossed with MIA144 to generate MIA217 *keyIs33; vsIs183 lite-1(ce314) lin-15(n765ts) X*.

728

729 **Ratiometric Ca^{2+} imaging**

730 Ratiometric Ca^{2+} imaging of the vulval muscles and VC neurons in freely behaving animals was
731 performed as previously described methods (Ravi, Nassar, et al., 2018). Late L4 hermaphrodites

732 were staged and then imaged 24 h later by being moved to an NGM agar chunk and a glass
733 coverslip being placed over. Animals were recorded on a Zeiss Axio Observer.Z1 inverted
734 compound microscope with a 20X 0.8NA Apochromat objective. Brightfield recordings of
735 behavior was recorded with infrared illumination using a FLIR Grasshopper 3 CMOS camera
736 after 2x2 binning using FlyCap software. Colibri.2 470 nm and 590 nm LEDs were used to co-
737 excite GCaMP5 and mCherry fluorescence which was captured at 20 Hz onto a Hamamatsu
738 ORCA Flash-4.0V2 sCMOS camera after channel separation using a Gemini image splitter. A
739 custom script in Bonsai was used to measure stage position at each frame of the recording which
740 was added to centroid position of the fluorescence object to measure animal speed in Ca^{2+}
741 imaging experiments (Lopes et al., 2015; Ravi, Nassar, et al., 2018). Each animal was recorded
742 until it entered an active egg-laying phase (up to 1 h), after which a 10-minute segment centered
743 around the onset of egg laying was extracted from the full recoding for analysis. Two-channel
744 fluorescence (GCaMP5/mCherry) image sequences were processed and analyzed in Fiji
745 (Schindelin et al., 2012), Volocity (PerkinElmer), and a custom script for MATLAB (MathWorks)
746 as previously described (Ravi, Nassar, et al., 2018).

747 Ratiometric Ca^{2+} imaging of the HSN neurons in freely behaving animals was performed as
748 previously described (Ravi, Garcia, et al., 2018). Late L4 hermaphrodites were staged and then
749 imaged 24 h later by being moved to an NGM agar chunk and a glass coverslip being placed
750 over. Animals were recorded on an inverted Leica TCS SP5 confocal microscope with a 20X
751 0.7NA Apochromat objective. 488 nm and 561 nm laser lines were used to co-excite GCaMP5
752 and mCherry fluorescence, respectively.

753

754 **Electrical silencing using HisCl**

Acute electrical silencing with histamine was performed as previously described (Pokala et al., 2014; Ravi, Garcia, et al., 2018). Animals were moved onto OP50-seeded NGM agar plates that contained either 0 mM or 10 mM histamine for four hours before the experiment.

Egg-laying behavior assays

The steady-state accumulation of eggs in the uterus was determined as previously described (Koelle & Horvitz, 1996). Briefly, late L4 hermaphrodites were staged onto OP50-seeded plates and grown at 20 °C for 30 h after which a single adult was placed into a 7 ul drop of 20% sodium hypochlorite (bleach) solution. The eggs, which are resistant to bleach, were then counted using a dissecting microscope. The timing of the first egg laid was assayed by staging a young adult (within 30 minutes of L4 to adult molt) animal onto an NGM agar plate with food and checking every following 30 minutes for the presence of an egg on the plate (Ravi, Garcia, et al., 2018).

Egg laying in liquid in response to exogenous serotonin was performed as described (Banerjee et al., 2017; Trent et al., 1983). Late L4 hermaphrodites were staged onto OP50-seed plates and grown at 20 °C for 24 h. Adult animals were placed singly into either 100 ul M9 buffer only or M9 buffer containing 18.5 mM serotonin creatinine sulfate salt (Sigma-Aldrich) in a 96-well microtiter dish. The number of eggs laid by each animal after 1 hour were then counted. Egg laying on plates in response to exogenous serotonin was performed on NGM agar infused with 18.5 mM serotonin creatine sulfate salt (Sigma-Aldrich). 3 animals were placed on each NGM agar plate and the number of eggs laid was counted after 1 hour and divided by 3 to calculate an average-animal response per plate.

Optogenetics

778 Optogenetic experiments with Channelrhodopsin-2 (ChR2) were performed using a Zeiss Axio
779 Observer.Z1 inverted compound microscope as previously described (Collins et al., 2016). ChR2
780 was excited in freely behaving animals using a 470 nm (blue) LED. Late L4 animals were staged
781 onto NGM agar plates seeded with *E. coli* OP50 bacterial cultures containing either 0.4 mM all-
782 *trans* retinal (ATR) or no ATR 24 h prior to the start of the experiment. Animals were then
783 continuously illuminated with blue light for 3-5 minutes and the locomotion behavior and number
784 of egg-laying events were recorded. For experiments combining optogenetics with ratiometric
785 Ca^{2+} imaging, the blue light would excite both the ChR2 and GCaMP5 fluorescence
786 simultaneously. Blue light intensity was chosen based on both optimal settings to observe robust
787 ChR2-activation and GCaMP5 fluorescence. Animals were excluded from a dataset if they
788 entered an active egg-laying state before the onset of blue light stimulation (one animal in total
789 across all experiments).

790

791 **Statistical analysis**

792 All data were analyzed using GraphPad Prism 8. Steady-state egg accumulation and timing of
793 first egg laid assays were compared using a one-way ANOVA with Bonferroni's correction for
794 multiple comparisons. Serotonin-induced egg laying assays were compared using either a
795 Kruskal-Wallis test with Dunn's correction for multiple comparisons (in buffer with individual
796 responses) or a one-way ANOVA with Bonferroni's correction for multiple comparisons (on
797 plates with averaged responses). Frequencies of inter-transient intervals were analyzed using
798 either a Kolmogorov-Smirnov test or Kruskal-Wallis test with Dunn's correction for multiple
799 comparisons. Proportion of failed egg-laying events was analyzed using a Mann-Whitney test.
800 Ca^{2+} imaging analyses of amplitude, transient peak amplitude, inter-transient interval, or

801 transient widths were compared using either a Student's t test or a one-way ANOVA with
802 Bonferroni's correction for multiple comparisons.

803

804 **Acknowledgements**

805 This work was funded by grants from the NIH (R01-NS086932) and NSF (IOS-1844657) to KMC.
806 RJK 3rd was supported by a University of Miami Maytag Fellowship. We thank David M. Miller III
807 for sharing plasmids. Some of the strains used in this study were provided by the *C.*
808 *elegans* Genetics Center, which is funded by NIH Office of Research Infrastructure Programs
809 (P40 OD010440). We thank Drs. Julia Dallman, Grace Zhai, Mason Klein, and members of the
810 Collins lab for helpful discussions and feedback on the manuscript.

811

812 **Table 1. Strain names and genotypes for all animals used in this study.**

Strain	Genotype	Feature	Reference
CB190	*unc-54(e190) I*	Myosin heavy chain null mutant	(Brenner, 1974)
LX1832	*lite-1(ce314) X lin-15(n765ts) X*	Blue light-resistant (optogenetics and Ca^{2+} imaging), multivulva (injection rescue marker)	(Collins & Koelle, 2013)
LX1918	*vsIs164 lite-1(ce314) lin-15(n765ts) X*	Vulval muscles expressing GCaMP5, mCherry	(Collins et al., 2016)
LX1960	*vsIs172; lite-1(ce314) lin-15(n765ts) X*	VC GCaMP5, mCherry	(Collins et al., 2016)
LX2004	*vsIs183 lite-1(ce314) lin-15(n765ts) X*	HSN expressing GCaMP5, mCherry	(Collins et al., 2016)
MIA116	*keyIs21; lite-1(ce314) lin-15(n765ts) X*	HSN HisCl	(Ravi, Garcia, et al., 2018)
MIA123	*egl-1(n986dm) V lite-1(ce314) lin-15(n765ts) X*	No HSNs	this study
MIA125	*keyIs23; lite-1(ce314) lin-15(n765ts) X*	VC HisCl	this study
MIA144	*keyIs33; lite-1(ce314) lin-15(n765ts) X*	VC Tetanus Toxin	this study
MIA146	*keyIs46; lite-1(ce314) lin-15(n765ts) X*	VC Tetanus Toxin	this study
MIA173	*keyIs46; egl-1(n986dm) V lite-1(ce314) lin-15(n765ts) X*	VC Tetanus Toxin; no HSNs	this study
MIA176	*keyIs23; egl-1(n986dm) V; lite-1(ce314) lin-15(n765ts) X*	VC HisCl; no HSNs	this study
MIA183	*keyIs33; vsIs164 lite-1(ce314) lin-15(n765ts) X*	VC Tetanus Toxin; vulval muscle GCaMP5, mCherry	this study
MIA217	*keyI33; vsIs183 lite-1(ce314) lin-15(n765ts) X*	VC Tetanus Toxin; HSN GCaMP5, mCherry	this study
MIA221	*keyIs3; vsIs164; lite-1(ce314) lin-15(n765ts) X*	VC Channelrhodopsin -2; vulval muscle GCaMP5, mCherry	this study
MIA229	*keyIs48; lite-1(ce314) lin-15(n765ts) X*	Vulval muscle Channelrhodopsin -2	this study
MIA241	*keyIs48; vsIs172; lite-1(ce314) lin-15(n765ts) X*	Vulval muscle Channelrhdopsin-2; VC GCaMP5, mCherry	this study
MIA250	*keyIs48; vsIs164 lite-1(ce314) lin-15(n765ts) X*	Vulval muscle Channelrhdopsin-2, GCaMP5, mCherry	this study

MIA298	*keyIs48; vsIs172; unc-54(e190) I; lite-1(ce314) lin-15(n765ts) X*	Vulval muscle Channelrhdopsin-2; VC GCaMP5, mCherry; *unc-54* myosin heavy chain null mutant background	this study
MIA26	*egl-1(n986dm) V*	No HSNs	(Ravi, Garcia, et al., 2018)
N2	*wild type*	Bristol wild-type strain	(Brenner, 1974)
LX1970	*wzIs30 IV; vsIs172; lite-1(ce314) lin-15(n765ts) X*	HSN Channelrhodopsin-2; VC GCaMP5, mCherry	(Collins et al., 2016)

813

References

Altun, Z. F., Chen, B., Wang, Z.-W., & Hall, D. H. (2009). High resolution map of Caenorhabditis elegans gap junction proteins. *Developmental Dynamics*, *238*(8), 1936–1950. https://doi.org/10.1002/dvdy.22025

Banerjee, N., Bhattacharya, R., Gorczyca, M., Collins, K. M., & Francis, M. M. (2017). Local neuropeptide signaling modulates serotonergic transmission to shape the temporal organization of C. elegans egg-laying behavior. *PLOS Genetics*, *13*(4), e1006697. https://doi.org/10.1371/journal.pgen.1006697

Bany, I. A., Dong, M.-Q., & Koelle, M. R. (2003). Genetic and Cellular Basis for Acetylcholine Inhibition of Caenorhabditis elegans Egg-Laying Behavior. *Journal of Neuroscience*, *23*(22), 8060–8069. https://doi.org/10.1523/JNEUROSCI.23-22-08060.2003

Bargmann, C. I. (2012). Beyond the connectome: How neuromodulators shape neural circuits. *BioEssays: News and Reviews in Molecular, Cellular and Developmental Biology*, *34*(6), 458–465. https://doi.org/10.1002/bies.201100185

Bargmann, C. I., & Marder, E. (2013). From the connectome to brain function. *Nature Methods*, *10*(6), 483–490. https://doi.org/10.1038/nmeth.2451

Bartussek, J., & Lehmann, F.-O. (2016). Proprioceptive feedback determines visuomotor gain in Drosophila. *Royal Society Open Science*, *3*(1). https://doi.org/10.1098/rsos.150562

Batista-García-Ramó, K., & Fernández-Verdecia, C. I. (2018). What We Know About the Brain Structure-Function Relationship. *Behavioral Sciences (Basel, Switzerland)*, *8*(4). https://doi.org/10.3390/bs8040039

Bentley, B., Branicky, R., Barnes, C. L., Chew, Y. L., Yemini, E., Bullmore, E. T., Vértes, P. E., & Schafer, W. R. (2016). The Multilayer Connectome of Caenorhabditis elegans. *PLoS Computational Biology*, *12*(12), e1005283. https://doi.org/10.1371/journal.pcbi.1005283

Brenner, S. (1974). The Genetics of CAENORHABDITIS ELEGANS. *Genetics*, *77*(1), 71–94.

839 Brewer, J. C., Olson, A. C., Collins, K. M., & Koelle, M. R. (2019). Serotonin and neuropeptides are
840 both released by the HSN command neuron to initiate Caenorhabditis elegans egg laying. *PLOS*
841 *Genetics*, *15*(1), e1007896. https://doi.org/10.1371/journal.pgen.1007896
842 Chase, D. L., Pepper, J. S., & Koelle, M. R. (2004). Mechanism of extrasynaptic dopamine signaling in
843 Caenorhabditis elegans. *Nature Neuroscience*, *7*(10), 1096–1103. https://doi.org/10.1038/nn1316
844 Clark, S. G., Lu, X., & Horvitz, H. R. (1994). The Caenorhabditis elegans locus lin-15, a negative
845 regulator of a tyrosine kinase signaling pathway, encodes two different proteins. *Genetics*,
846 *137*(4), 987–997.
847 Collins, K. M., Bode, A., Fernandez, R. W., Tanis, J. E., Brewer, J. C., Creamer, M. S., & Koelle, M. R.
848 (2016). Activity of the C. elegans egg-laying behavior circuit is controlled by competing
849 activation and feedback inhibition. *ELife*, *5*, e21126. https://doi.org/10.7554/eLife.21126
850 Collins, K. M., & Koelle, M. R. (2013). Postsynaptic ERG potassium channels limit muscle excitability
851 to allow distinct egg-laying behavior states in Caenorhabditis elegans. *The Journal of*
852 *Neuroscience: The Official Journal of the Society for Neuroscience*, *33*(2), 761–775.
853 https://doi.org/10.1523/JNEUROSCI.3896-12.2013
854 Cook, S. J., Jarrell, T. A., Brittin, C. A., Wang, Y., Bloniarz, A. E., Yakovlev, M. A., Nguyen, K. C. Q.,
855 Tang, L. T.-H., Bayer, E. A., Duerr, J. S., Bülow, H. E., Hobert, O., Hall, D. H., & Emmons, S.
856 W. (2019). Whole-animal connectomes of both Caenorhabditis elegans sexes. *Nature*,
857 *571*(7763), 63–71. https://doi.org/10.1038/s41586-019-1352-7
858 Dittman, J. S., & Kaplan, J. M. (2008). Behavioral impact of neurotransmitter-activated G-protein-
859 coupled receptors: Muscarinic and GABAB receptors regulate Caenorhabditis elegans
860 locomotion. *The Journal of Neuroscience: The Official Journal of the Society for Neuroscience*,
861 *28*(28), 7104–7112. https://doi.org/10.1523/JNEUROSCI.0378-08.2008

862 Donnelly, J. L., Clark, C. M., Leifer, A. M., Pirri, J. K., Haburcak, M., Francis, M. M., Samuel, A. D. T.,
863 & Alkema, M. J. (2013). Monoaminergic Orchestration of Motor Programs in a Complex C.
864 elegans Behavior. *PLOS Biology*, *11*(4), e1001529. https://doi.org/10.1371/journal.pbio.1001529
865 Duerr, J. S., Gaskin, J., & Rand, J. B. (2001). Identified neurons in C. elegans coexpress vesicular
866 transporters for acetylcholine and monoamines. *American Journal of Physiology. Cell*
867 *Physiology*, *280*(6), C1616-1622. https://doi.org/10.1152/ajpcell.2001.280.6.C1616
868 Duerr, J. S., Han, H.-P., Fields, S. D., & Rand, J. B. (2008). Identification of major classes of
869 cholinergic neurons in the nematode Caenorhabditis elegans. *Journal of Comparative Neurology*,
870 *506*(3), 398–408. https://doi.org/10.1002/cne.21551
871 Emtage, L., Aziz-Zaman, S., Padovan-Merhar, O., Horvitz, H. R., Fang-Yen, C., & Ringstad, N. (2012).
872 IRK-1 Potassium Channels Mediate Peptidergic Inhibition of Caenorhabditis elegans Serotonin
873 Neurons via a Go Signaling Pathway. *Journal of Neuroscience*, *32*(46), 16285–16295.
874 https://doi.org/10.1523/JNEUROSCI.2667-12.2012
875 Fang, Y., Nakashima, R., Matsumiya, K., Kuriki, I., & Shioiri, S. (2015). Eye-Head Coordination for
876 Visual Cognitive Processing. *PLoS ONE*, *10*(3). https://doi.org/10.1371/journal.pone.0121035
877 Fernandez, R. W., Wei, K., Wang, E. Y., Mikalauskaite, D., Olson, A., Pepper, J., Christie, N., Kim, S.,
878 & Koelle, M. R. (2020). Cellular expression and functional roles of all 26 neurotransmitter
879 GPCRs in the C. elegans egg-laying circuit. *BioRxiv*, 2020.04.23.037242.
880 https://doi.org/10.1101/2020.04.23.037242
881 Hapiak, V. M., Hobson, R. J., Hughes, L., Smith, K., Harris, G., Condon, C., Komuniecki, P., &
882 Komuniecki, R. W. (2009). Dual Excitatory and Inhibitory Serotonergic Inputs Modulate Egg
883 Laying in Caenorhabditis elegans. *Genetics*, *181*(1), 153–163.
884 https://doi.org/10.1534/genetics.108.096891

885 Hardaker, L. A., Singer, E., Kerr, R., Zhou, G., & Schafer, W. R. (2001). Serotonin modulates
886 locomotory behavior and coordinates egg-laying and movement in Caenorhabditis elegans.
887 *Journal of Neurobiology*, *49*(4), 303–313. https://doi.org/10.1002/neu.10014
888 Hobson, R. J., Hapiak, V. M., Xiao, H., Buehrer, K. L., Komuniecki, P. R., & Komuniecki, R. W.
889 (2006). SER-7, a Caenorhabditis elegans 5-HT7-like Receptor, Is Essential for the 5-HT
890 Stimulation of Pharyngeal Pumping and Egg Laying. *Genetics*, *172*(1), 159–169.
891 https://doi.org/10.1534/genetics.105.044495
892 Jose, A. M., Bany, I. A., Chase, D. L., & Koelle, M. R. (2007). A Specific Subset of Transient Receptor
893 Potential Vanilloid-Type Channel Subunits in Caenorhabditis elegans Endocrine Cells Function
894 as Mixed Heteromers to Promote Neurotransmitter Release. *Genetics*, *175*(1), 93–105.
895 https://doi.org/10.1534/genetics.106.065516
896 Kim, J., Poole, D. S., Waggoner, L. E., Kempf, A., Ramirez, D. S., Treschow, P. A., & Schafer, W. R.
897 (2001). Genes affecting the activity of nicotinic receptors involved in Caenorhabditis elegans
898 egg-laying behavior. *Genetics*, *157*(4), 1599–1610.
899 Koelle, M. R. (2018). Neurotransmitter signaling through heterotrimeric G proteins: Insights from
900 studies in C. elegans. *WormBook : The Online Review of C. Elegans Biology*.
901 https://doi.org/10.1895/wormbook.1.75.2
902 Koelle, M. R., & Horvitz, H. R. (1996). EGL-10 regulates G protein signaling in the C. elegans nervous
903 system and shares a conserved domain with many mammalian proteins. *Cell*, *84*(1), 115–125.
904 https://doi.org/10.1016/s0092-8674(00)80998-8
905 Lerner, T. N., Ye, L., & Deisseroth, K. (2016). Communication in Neural Circuits: Tools, Opportunities,
906 and Challenges. *Cell*, *164*(6), 1136–1150. https://doi.org/10.1016/j.cell.2016.02.027
907 Li, P., Collins, K. M., Koelle, M. R., & Shen, K. (2013). LIN-12/Notch signaling instructs postsynaptic
908 muscle arm development by regulating UNC-40/DCC and MADD-2 in Caenorhabditis elegans.
909 *ELife*, *2*. https://doi.org/10.7554/eLife.00378

910 Lopes, G., Bonacchi, N., Frazão, J., Neto, J. P., Atallah, B. V., Soares, S., Moreira, L., Matias, S.,
911 Itskov, P. M., Correia, P. A., Medina, R. E., Calcaterra, L., Dreosti, E., Paton, J. J., & Kampff, A.
912 R. (2015). Bonsai: An event-based framework for processing and controlling data streams.
913 *Frontiers in Neuroinformatics*, *9*, 7. https://doi.org/10.3389/fninf.2015.00007
914 Lukos, J. R., Snider, J., Hernandez, M. E., Tunik, E., Hillyard, S., & Poizner, H. (2013). Parkinson's
915 disease patients show impaired corrective grasp control and eye-hand coupling when reaching to
916 grasp virtual objects. *Neuroscience*, *254*, 205–221.
917 https://doi.org/10.1016/j.neuroscience.2013.09.026
918 Meinertzhagen, I. A. (2018). Of what use is connectomics? A personal perspective on the Drosophila
919 connectome. *The Journal of Experimental Biology*, *221*(Pt 10).
920 https://doi.org/10.1242/jeb.164954
921 Pereira, L., Kratsios, P., Serrano-Saiz, E., Sheftel, H., Mayo, A. E., Hall, D. H., White, J. G., LeBoeuf,
922 B., Garcia, L. R., Alon, U., & Hobert, O. (2015). A cellular and regulatory map of the
923 cholinergic nervous system of C. elegans. *ELife*, *4*, e12432. https://doi.org/10.7554/eLife.12432
924 Pirri, J. K., McPherson, A. D., Donnelly, J. L., Francis, M. M., & Alkema, M. J. (2009). A tyramine-
925 gated chloride channel coordinates distinct motor programs of a Caenorhabditis elegans escape
926 response. *Neuron*, *62*(4), 526–538. https://doi.org/10.1016/j.neuron.2009.04.013
927 Pokala, N., Liu, Q., Gordus, A., & Bargmann, C. I. (2014). Inducible and titratable silencing of
928 Caenorhabditis elegans neurons in vivo with histamine-gated chloride channels. *Proceedings of*
929 *the National Academy of Sciences*, *111*(7), 2770–2775. https://doi.org/10.1073/pnas.1400615111
930 Ravi, B., Garcia, J., & Collins, K. M. (2018). Homeostatic Feedback Modulates the Development of
931 Two-State Patterned Activity in a Model Serotonin Motor Circuit in Caenorhabditis elegans.
932 *Journal of Neuroscience*, *38*(28), 6283–6298. https://doi.org/10.1523/JNEUROSCI.3658-
933 17.2018

Ravi, B., Nassar, L. M., Kopchock, R. J., III, Dhakal, P., Scheetz, M., & Collins, K. M. (2018). Ratiometric Calcium Imaging of Individual Neurons in Behaving Caenorhabditis Elegans. *JoVE (Journal of Visualized Experiments)*, *132*, e56911. https://doi.org/10.3791/56911

Richmond, J. E., & Jorgensen, E. M. (1999). One GABA and two acetylcholine receptors function at the C. elegans neuromuscular junction. *Nature Neuroscience*, *2*(9), 791–797. https://doi.org/10.1038/12160

Schafer, W. R. (2006). Genetics of Egg-Laying in Worms. *Annual Review of Genetics*, *40*(1), 487–509. https://doi.org/10.1146/annurev.genet.40.110405.090527

Schafer, W. R., Sanchezt, B. M., & Kenyon, C. (1996). *Genes Affecting Sensitivity to Serotonin in Caenorhabditis elegans*. 12.

Schindelin, J., Arganda-Carreras, I., Frise, E., Kaynig, V., Longair, M., Pietzsch, T., Preibisch, S., Rueden, C., Saalfeld, S., Schmid, B., Tinevez, J.-Y., White, D. J., Hartenstein, V., Eliceiri, K., Tomancak, P., & Cardona, A. (2012). Fiji: An open-source platform for biological-image analysis. *Nature Methods*, *9*(7), 676–682. https://doi.org/10.1038/nmeth.2019

Sengupta, P., & Samuel, A. D. T. (2009). C. elegans: A model system for systems neuroscience. *Current Opinion in Neurobiology*, *19*(6), 637–643. https://doi.org/10.1016/j.conb.2009.09.009

Shyn, S. I., Kerr, R., & Schafer, W. R. (2003). Serotonin and Go Modulate Functional States of Neurons and Muscles Controlling C. elegans Egg-Laying Behavior. *Current Biology*, *13*(21), 1910–1915. https://doi.org/10.1016/j.cub.2003.10.025

Song, B., Faumont, S., Lockery, S., & Avery, L. (2013). Recognition of familiar food activates feeding via an endocrine serotonin signal in Caenorhabditis elegans. *ELife*, *2*. https://doi.org/10.7554/eLife.00329

Trent, C., Tsuing, N., & Horvitz, H. R. (1983). Egg-laying defective mutants of the nematode Caenorhabditis elegans. *Genetics*, *104*(4), 619–647.

958 Trojanowski, N. F., Raizen, D. M., & Fang-Yen, C. (2016). Pharyngeal pumping in Caenorhabditis
959 elegans depends on tonic and phasic signaling from the nervous system. *Scientific Reports*, *6*(1),
960 22940. https://doi.org/10.1038/srep22940
961 Waggoner, L. E., Dickinson, K. A., Poole, D. S., Tabuse, Y., Miwa, J., & Schafer, W. R. (2000). Long-
962 term nicotine adaptation in Caenorhabditis elegans involves PKC-dependent changes in nicotinic
963 receptor abundance. *The Journal of Neuroscience: The Official Journal of the Society for*
964 *Neuroscience*, *20*(23), 8802–8811.
965 Waggoner, L. E., Zhou, G. T., Schafer, R. W., & Schafer, W. R. (1998). Control of Alternative
966 Behavioral States by Serotonin in Caenorhabditis elegans. *Neuron*, *21*(1), 203–214.
967 https://doi.org/10.1016/S0896-6273(00)80527-9
968 Walker, D. S., & Schafer, W. R. (2020). Distinct roles for innexin gap junctions and hemichannels in
969 mechanosensation. *ELife*, *9*, e50597. https://doi.org/10.7554/eLife.50597
970 White, J. G., Southgate, E., Thomson, J. N., & Brenner, S. (1986). The structure of the nervous system
971 of the nematode Caenorhabditis elegans. *Philosophical Transactions of the Royal Society of*
972 *London. Series B, Biological Sciences*, *314*(1165), 1–340. https://doi.org/10.1098/rstb.1986.0056
973 Xiao, H., Hapiak, V. M., Smith, K. A., Lin, L., Hobson, R. J., Plenefisch, J., & Komuniecki, R. (2006).
974 SER-1, a Caenorhabditis elegans 5-HT2-like receptor, and a multi-PDZ domain containing
975 protein (MPZ-1) interact in vulval muscle to facilitate serotonin-stimulated egg-laying.
976 *Developmental Biology*, *298*(2), 379–391. https://doi.org/10.1016/j.ydbio.2006.06.044
977 Yeon, J., Kim, J., Kim, D.-Y., Kim, H., Kim, J., Du, E. J., Kang, K., Lim, H.-H., Moon, D., & Kim, K.
978 (2018). A sensory-motor neuron type mediates proprioceptive coordination of steering in C.
979 elegans via two TRPC channels. *PLOS Biology*, *16*(6), e2004929.
980 https://doi.org/10.1371/journal.pbio.2004929
981 Zhang, M., Chung, S. H., Fang-Yen, C., Craig, C., Kerr, R. A., Suzuki, H., Samuel, A. D. T., Mazur, E.,
982 & Schafer, W. R. (2008). A self-regulating feed-forward circuit controlling C. elegans egg-

laying behavior. *Current Biology: CB*, *18*(19), 1445–1455. https://doi.org/10.1016/j.cub.2008.08.047

Zhang, M., Schafer, W. R., & Breitling, R. (2010). A circuit model of the temporal pattern generator of Caenorhabditis egg-laying behavior. *BMC Systems Biology*, *4*(1), 81. https://doi.org/10.1186/1752-0509-4-81

Zhen, M., & Samuel, A. D. (2015). C. elegans locomotion: Small circuits, complex functions. *Current Opinion in Neurobiology*, *33*, 117–126. https://doi.org/10.1016/j.conb.2015.03.009